LONGITUDINAL IMPACT OF A THIN VISCOELASTIC ROD

Thesis for the Degree of Ph. D.

MICHIGAN STATE UNIVERSITY

Douglas Monroe Norris, Jr.

1962

This is to certify that the

thesis entitled

Longitudinal

Impact of a Thin Viscoelastic Rod

presented by

Douglas Monroe Norris, Jr.

has been accepted towards fulfillment
of the requirements for

Ph.D. degree in Applied Mechanics

George E. Mase
Major professor

Date May 18, 1962

O-169

ABSTRACT

LONGITUDINAL IMPACT OF A THIN VISCOELASTIC ROD

by Douglas Monroe Norris, Jr.

The propagation of stress pulses in a semi-infinite viscoelastic rod is investigated. A thin rod of polyethylene is axially impacted and the stress condition on the end measured as a function of time. The resulting longitudinal strain in the bar is simultaneously monitored at a number of positions along the bar.

The equations describing the resulting motion are presented and the solution given by Fourier transform methods for the case of a material obeying the Bolzmann superposition law. The solutions are numerically evaluated for the experimental stress boundary condition using the complex compliance measured from sinusoidal vibration tests on fibers of the same material. Strain at positions along the bar is also computed using strain measured at another position on the bar as the boundary condition.

The results for these two conditions are compared with the experimentally obtained results. The agreement is good.

LONGITUDINAL IMPACT OF A THIN VISCOELASTIC ROD

By

Douglas Monroe Norris, Jr.

A THESIS

Submitted to
Michigan State University
in partial fulfillment of the requirements
for the degree of

DOCTOR OF PHILOSOPHY

Department of Applied Mechanics

.

1962

ACKNOWLEDGMENTS

I wish to thank Professor George E. Mase for his help throughout this project. I wish also to thank Professor L. E. Malvern for his suggestion of the problem and his significant contributions toward its solution. Appreciation is also given to Professor C. A. Tatro for his counsel in various aspects of the experimental work and to Professor Charles P. Wells and Professor William A. Bradley for their service on my graduate committee.

I wish to thank Mr. J. W. Hoffman, Director of the Division of Engineering Research, for making available various services and funds and the E. I. du Pont de Nemours & Company for furnishing the experimental materials.

Appreciation is also due to the National Science Foundation for the Science Faculty Fellowship under which the work was made possible.

****

TABLE OF CONTENTS

LIST OF TABLES

TABLE Page

LIST OF FIGURES

FIGURE

Page

LIST OF APPENDICES

I. INTRODUCTION

Recent technological developments have motivated extensive interest in problems of response of viscoelastic structures to dynamic loading. A number of analytic solutions have been given for the case of stress pulse propagation in a thin rod subjected to an axial impact applied to one end. However, relatively little experimental work has been undertaken in this area. The purpose of this dissertation is to experimentally and analytically investigate the transient phenomenon associated with the propagation of a stress pulse in a semi-infinite viscoelastic bar.

The work falls into two general areas. The first area is an experimental investigation of the stress pulse propagation phenomenon. The second area is a combination of analytical and experimental work which presents the numerical results of a theory describing the stress pulse propagation phenomenon in a particular viscoelastic material. The conclusions drawn from the comparison of these results constitute the major contribution of this thesis.

In the experimental investigation the end of a thin rod of polyethylene is given an axial impact. The impact is maintained and the consequent end stress is measured as a function of time. The resulting strain wave is simultaneously monitored at a number of positions along the bar. The data obtained from these measurements extend the experimental results of Kolsky [1956][1] to give a more complete description of impact phenomenon. Kolsky's work was limited to an impulse end condition.

The second purpose of this dissertation is to compute the strain using the equations of the one dimensional elementary theory of viscoelastic

---

[1]Numbers in the brackets refer to the Bibliography at the end of the paper.

wave propagation. The theory used is essentially that developed by Hunter [1960] for a viscoelastic material obeying a Bolzmann superposition stress strain law. It is necessary to perform additional experimentation to determine the viscoelastic material properties needed in evaluating integral solutions to the strain pulse propagation problem. These material properties are determined by sinusoidal vibration tests on fibers of the material.

The Boltzmann superposition law may be taken as the fundamental relationship defining a linear viscoelastic material. More generally, a viscoelastic material may be defined as one in which the stress strain relationship is dependent on time. For example, such a material when loaded may have an instantaneous deflection followed by a continued elongation as time passes. Upon removal of the load the material might partially recover elastically and then gradually recover to the original length or might maintain a permanent deformation. These effects might happen quite rapidly in time or over a number of years. Creep and relaxation are two particular characteristics of a viscoelastic solid.

Viscoelastic materials have other characteristics not found in purely elastic media. One factor that complicates an analysis is that the viscoelastic material is dispersive. This means that sinusoidal waves of one frequency are propagated at a different velocity from that of another frequency. The net effect of this phenomenon is that a strain pulse will constantly change in shape as it moves through a viscoelastic solid. Further complication arises from the fact that waves of higher frequency are attenuated more rapidly than waves of lower frequency. It is this combination of dispersion and attenuation which makes the analysis of viscoelastic materials more complicated than analysis in purely Hookean media and has recently attracted much attention to the problem.

II. HISTORY

A brief history of impact in viscoelastic solids is given here. Discussion of static analysis, sinusoidal response and other work done on viscoelastic materials will be only briefly mentioned since the primary purpose is the analysis of transient effects. The reader interested in the general theory of viscoelasticity is referred to books by Bland [1960], Gross [1953], Bergen [1960], and Alfrey [1948].

An early mention of time dependent material effects was given by Weber [1835]. He described an "elastische Nachwirkung" in silk fibers and arrived at an empirical equation relating displacement and time. Thompson [1933] gave a summary of the developments in the field up to the date of his paper. Most of the early work was concerned with formulation of viscoelastic stress strain laws. This paper by Thompson gave the first solution to an impact problem, a torsional ramp function pulse in a Voigt cylinder.

The period following the second world war produced extensive work in viscoelastic analysis in statically deformed bodies. Alfrey's book in 1948 followed by Tsien's paper in 1950 extended the great quantity of elastic solutions to viscoelastic media by the now well-known correspondence principle.

In the area of wave propagation, Ricker [1943] considered the problem of a sharp pulse propagated in what actually amounted to a Voigt solid in connection with a seismic problem. A survey of the literature in viscoelastic wave propagation is given by Kolsky [1958] and Hunter [1960].

Serious analytic interest in the wave propagation problem seemed to originate in 1951 with papers by Zverev [1951] and Malvern [1951]. Zverev solved the problem for a semi-infinite bar of Voigt material with a suddenly applied end velocity by the use of the Laplace transform. Malvern,in investigating strain rate effects in plastic wave propagation, obtained a formal solution for a propagation problem in a Maxwell medium. This particular solution was a special case of a more general plastic wave theory.

These two papers were quickly followed by four other papers discussing the same problem by other methods and for other materials. Lee and Kanter [1953] obtained solutions for pulse propagation in a Maxwell material. Glauz and Lee [1954] obtained the solution to the problem for a material representable by a four parameter model using the method of characteristics. Morrison [1956] used the Laplace transform to obtain the solution in a Voigt and three parameter material. A comparison of these last three papers is given by Lee and Morrison [1956].

A more general constitutive relationship may be chosen in the form of a Boltzmann superposition integral. The theory is well developed by Leaderman [1943] and Gross [1953]. An interesting paper on pulse propagation in a simplified hereditary material was given by Eubanks, Muster and Volterra [1954]. Using the superposition law Berry and Hunter [1955] solved the wave problem for a number of different boundary conditions using the Laplace transform. Similar approaches were given by Sips [1951a, b] and Charles [1951]. More recently, Hunter [1960] discussed wave propagation in viscoelastic materials including important work on Fourier transform methods of special interest to the experimentalist. Books by Kolsky [1953] and Bland [1960] include material on particular problems in viscoelastic impact.

Experimental work in the field of viscoelastic waves is limited. It would seem that most of the work on longitudinal impact has been done by Kolsky and his associates. Kolsky [1953] determined dynamic stress strain curves for polymers by longitudinal impact applied for times in the order of 20 microseconds. Propagation of very short strain pulses in rods of viscoelastic material was investigated by Kolsky [1956] in another important paper. The particular experimental problem treated here was motivated by this work.

In Kolsky's 1956 paper an integral expression for the displacement in an impacted semi-infinite viscoelastic rod was given. The integral was valid only for the case where the impact was representable by a Dirac delta function. Using the experimental data of Hillier [1949] for the dispersion and attenuation effects, Kolsky was able to numerically evaluate this integral. He thus analytically predicted the displacement as a function of time at any point on the bar for a sharp impact on the end of the bar. The results were checked experimentally using explosive charges to generate the short pulse of about 2 microseconds duration. The results were compared and are discussed in more detail later in this thesis.

The problem treated in this thesis extends Kolsky's results to the case of a much longer initially applied arbitrary stress pulse. The analysis of the finite pulse considerably complicates both the mathematical analysis and the experimental techniques necessary to verify the theory. Details of the methods used in this work are given in the next section.

Bodner and Kolsky [1958] extended Kolsky's 1956 impulse method to lead bars which were shown to behave viscoelastically. Experimental results were compared with computed results and a good correspondence was found. This was surprising since the analysis assumed linearity which was demonstrated not to exist.

The reader interested in experimentation should also see two other review articles, Kolsky [1959] and Kolsky [1960]. More recently, Hillier [1961] has reviewed methods of measurement of dynamic viscoelastic moduli by sinusoidal and pulse techniques. An excellent bibliography is included.

III. DESCRIPTION OF THE PROBLEM

The elementary theory of elastic wave propagation predicts that a strain pulse traveling in an elastic bar will remain undistorted as it moves along the bar. A strain pulse traveling in a viscoelastic bar is both attenuated and dispersed as it moves along the bar. The objective of this study is to analytically and experimentally investigate the phenomenological behavior of a longitudinal strain pulse as it travels in an impacted bar of viscoelastic material. The one-dimensional elementary wave propagation theory is used.

A more exact elastic theory was developed by Pochammer [1876] and Chree [1886] (see Love [1927] p. 287 et seq.) for an infinite circular cylinder free from traction. It was shown that the velocity of propagation of a sinusoidal wave along the cylinder actually depends on the ratio of the wavelength, say λ to the cylinder diameter, a, and that

$$v \rightarrow \left(\frac{E}{\rho}\right)^{\frac{1}{2}} \qquad \text{as} \qquad \frac{\lambda}{a} \rightarrow \infty .$$

Actually, Davies [1948] has shown if $\frac{\lambda}{a} > 10$ this type of dispersion, called geometric dispersion, is not significant. However, in a complete analysis it is necessary to consider both this geometric dispersion and dispersion due to viscoelastic material properties. This involves mathematical difficulties and the problem has not yet been solved. Kolsky [1956], using the delta function strain pulse, has attributed a difference in his computed and experimental data to the effect of this geometric dispersion.

The problem of geometric dispersion is difficult to separate from the natural dispersion inherent in the material. However, the geometric dispersion may be minimized by using a pulse loading whose frequency spectrum is largely composed of low frequency components having associated long wavelengths. This is the procedure to be followed here; the boundary stress pulse is made approximately 500 microseconds in length and the dispersion is considered to be that of the material. This is not strictly true, of course, but is a better approximation than that possible with a shorter pulse.

We consider the case of the propagation of longitudinal waves in a semi-infinite viscoelastic rod $x \geq 0$. Let $u(x, t)$ denote the displacement of the section x of the rod at time t, so that its position is given as $(u + x)$. Let $\sigma(x, t)$ and $\epsilon(x, t)$ denote the stress and strain respectively which will be assumed uniform across the rod at position x. Then from the elementary one-dimensional theory of wave propagation we have

$$\rho \frac{\partial^2 u}{\partial t^2} = \frac{\partial \sigma}{\partial x} \tag{1}$$

$$\epsilon = \frac{\partial u}{\partial x} \tag{2}$$

where ρ is the density of the material in the unstrained state.

The stress strain relation is taken in the form of a superposition integral

$$\sigma(t) = E_D \left\{ \epsilon(t) - \int_{-\infty}^{t} \frac{d\epsilon(\tau)}{d\tau} \phi(t-\tau) d\tau \right\} \tag{3}$$

where E_D is the dynamic Young's modulus and $\phi(t)$ is the relaxation function. $\phi(t)$ may be determined by a uniaxial relaxation test. Equation (3) is derived by considering the stress response to an instantaneously applied Heaviside strain step on the uniaxial bar which is then generalized to an arbitrary strain loading by the superposition integral. The details on the derivation of this equation and the following solution of Equations (1), (2) and (3) are given in Appendix I. These three equations plus the particular boundary and initial conditions represent the complete description of the wave propagation phenomena in the viscoelastic rod. The boundary condition considered here is one of stress, $\sigma(0, t)$, prescribed at the end of a semi-infinite rod.

The stress pulse may be represented by a Fourier transform as the superposition of a spectrum of sinusoidal waves of angular frequency ω. It has already been mentioned that in viscoelastic materials each of these frequencies is propagated at a different velocity. This velocity is called the phase velocity $c(\omega)$. Each frequency component is also attenuated as it moves down the bar. Let this damping coefficient be denoted $a(\omega)$ with units of per inch.

The solution of Equations (1), (2) and (3) is effected in a manner similar to that given by Hunter [1960] by the one-sided Fourier transform subject to the conditions

$$u(x, o) = \frac{\partial u}{\partial t}(x, o) = 0 \qquad x \geq 0$$

$$\left.\begin{aligned} &\sigma(0, t) = f(t) \\ &\lim_{x \to \infty} \sigma(x, t) = 0 \end{aligned}\right\} \quad t > 0 \tag{4}$$

yielding

$$\pi\epsilon(x, t) = \int_0^\infty \exp[-a(\omega)x]\left\{A(\omega)\cos[\omega(t - \frac{x}{c})] + B(\omega)\sin[\omega(t - \frac{x}{c})]\right\}d\omega$$

$$A(\omega) = \frac{1}{\rho[c(\omega)]^2}\left[\bar{\sigma}_R - \frac{2a(\omega)c(\omega)}{\omega}\bar{\sigma}_I\right] \tag{5}$$

$$B(\omega) = \frac{1}{\rho[c(\omega)]^2}\left[\bar{\sigma}_I + \frac{2a(\omega)c(\omega)}{\omega}\bar{\sigma}_R\right]$$

$$\bar{\sigma}_R = \int_0^\infty \sigma(0, t)\cos\omega t\,dt \qquad \bar{\sigma}_I = \int_0^\infty \sigma(0, t)\sin\omega t\,dt.$$

Thus if the boundary stress condition, $\sigma(0, t)$, is known and $a(\omega)$ and $c(\omega)$ are given over a sufficient frequency range, the resulting strain in the bar may be calculated by evaluating Equation (5).

In a similar manner for the conditions

$$\epsilon(x, o) = \frac{\partial \epsilon}{\partial t}(x, o) = 0 \qquad x \geq 0$$

$$\left.\begin{aligned} \epsilon(0, t) &= g(t) \\ \lim_{x \to \infty} \epsilon(x, t) &= 0 \end{aligned}\right\} \qquad t > 0,$$

the solution of Equations (1), (2) and (3) may be shown to yield

$$\pi\epsilon(x, t) = \int_0^\infty \exp\left[-\alpha(\omega)x\right]\left\{ \bar{\epsilon}_R \cos[\omega(t-\frac{x}{c})] + \bar{\epsilon}_I \sin[\omega(t-\frac{x}{c})] \right\} d\omega$$

$$\bar{\epsilon}_R = \int_0^\infty \epsilon(0, t)\cos\omega t dt \qquad \bar{\epsilon}_I = \int_0^\infty \epsilon(0, t)\sin\omega t dt. \tag{6}$$

Rather than measure the strain $\epsilon(0, t)$ as a boundary condition, Equation (6) may be used (as is later done) to predict strain at, say position x_2 if the strain as a function of time is known at some other position, say x_1. Again, the two quanties $\alpha(\omega)$ and $c(\omega)$ which completely describe the material properties must first be determined.

The particular problem which is considered here is to evaluate Equations (5) and (6) for some particular viscoelastic material and to compare the solution with the experimentally measured strain in the bar. To do this the following information must be experimentally obtained:

a. the phase velocity and the damping coefficient over the significant part of the frequency spectrum,
b. the 500 microsecond boundary stress condition, $\sigma(0, t)$,
c. the experimental strain, $\epsilon(x, t)$, in the polymer bar at a representative number of points on the bar to compare with the solution of Equations (5) and (6).

The material selected for this work was a low density polyethylene number B8020 manufactured by the E. I. du Pont de Nemours and Company. This material is chemically quite similar to the polyethylene used by Kolsky [1956] which was manufactured by the Imperial Chemical Industries Limited and is presently designated Alkathene WRM 19. Unfortunately, this same material was not available in this country. Since it was thought desirable for comparison purposes to use a chemically similar material, du Pont was requested to supply a similar polymer. The material is physically a translucent, milky white, quite flabby polymer. It has a melt index of 23, a density of 0.915 grams per square centimeter and crystalline melting temperature between 115° and 120° C. It presently has typical application in coaxial cable dielectric, flexible bottles, ice cube trays and packaging film.

IV. SUMMARY OF THE EXPERIMENTAL WORK

The material damping $\alpha(\omega)$ and phase velocity $c(\omega)$ were determined by longitudinal sinusoidal vibration tests on unoriented fibers of polyethylene. These fibers varied in length from 47 inches to 24 feet and had a diameter of 0.030 inches. One end was driven longitudinally by a phonograph cutter head. The amplitude and phase of the traveling wave was monitored as a function of distance (usually every inch) at each frequency by a conventional ceramic phonograph crystal pickup lightly touching the fiber. Knowing the phase difference and amplitude ratio of the input and output signal it was possible to calculate the damping and velocity at each frequency. The method used was similar to that employed by Ballou and Smith [1949] and Hillier and Kolsky [1949]. The details are given in Appendix II.

It was found over the frequency range considered that the damping could be accurately represented by

$$\alpha(\omega) = 2.753 \times 10^{-6}\, \omega \tag{7}$$

as shown in Appendix II. The phase velocity is given in Figure 1.

The impact tests were made using a modified Hopkinson-Davies pressure bar as developed by Davies [1948]. Figure 2 illustrates the experimental arrangement used in the long pulse impact tests. The firing device is a commercial Hyge Shock Tester, type HY-3433, manufactured by Consolidated Electrodynamics Corporation. The complete mechanical system is composed of this accelerating device, two long cylindrical magnesium rods called the "striker" bar and the "transmitter" bar respectively, the polymer sample bar and finally a stopping device. All rods were 1/2 inch diameter. The bar system is mounted horizontally

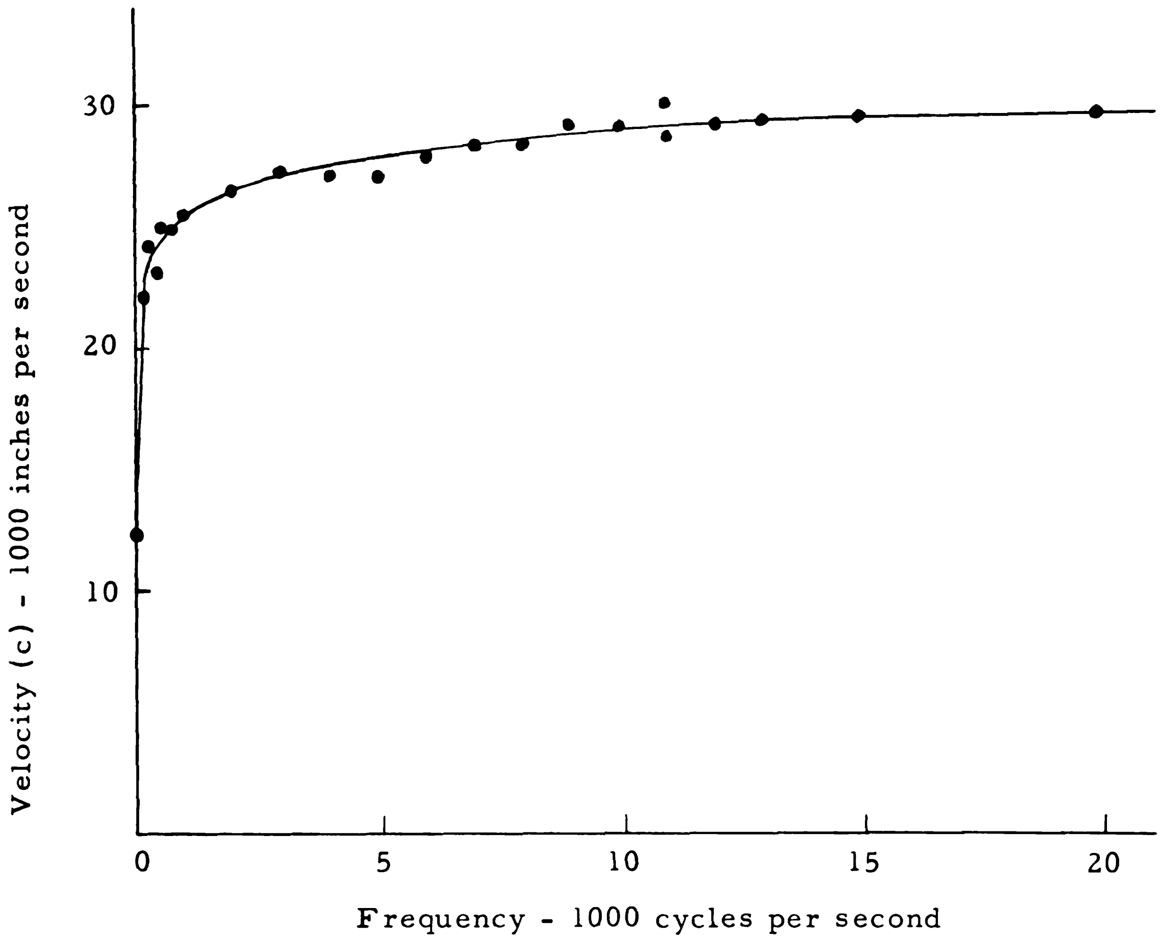

Figure 1. Experimental measurement of velocity of sound in polyethylene at 75°F.

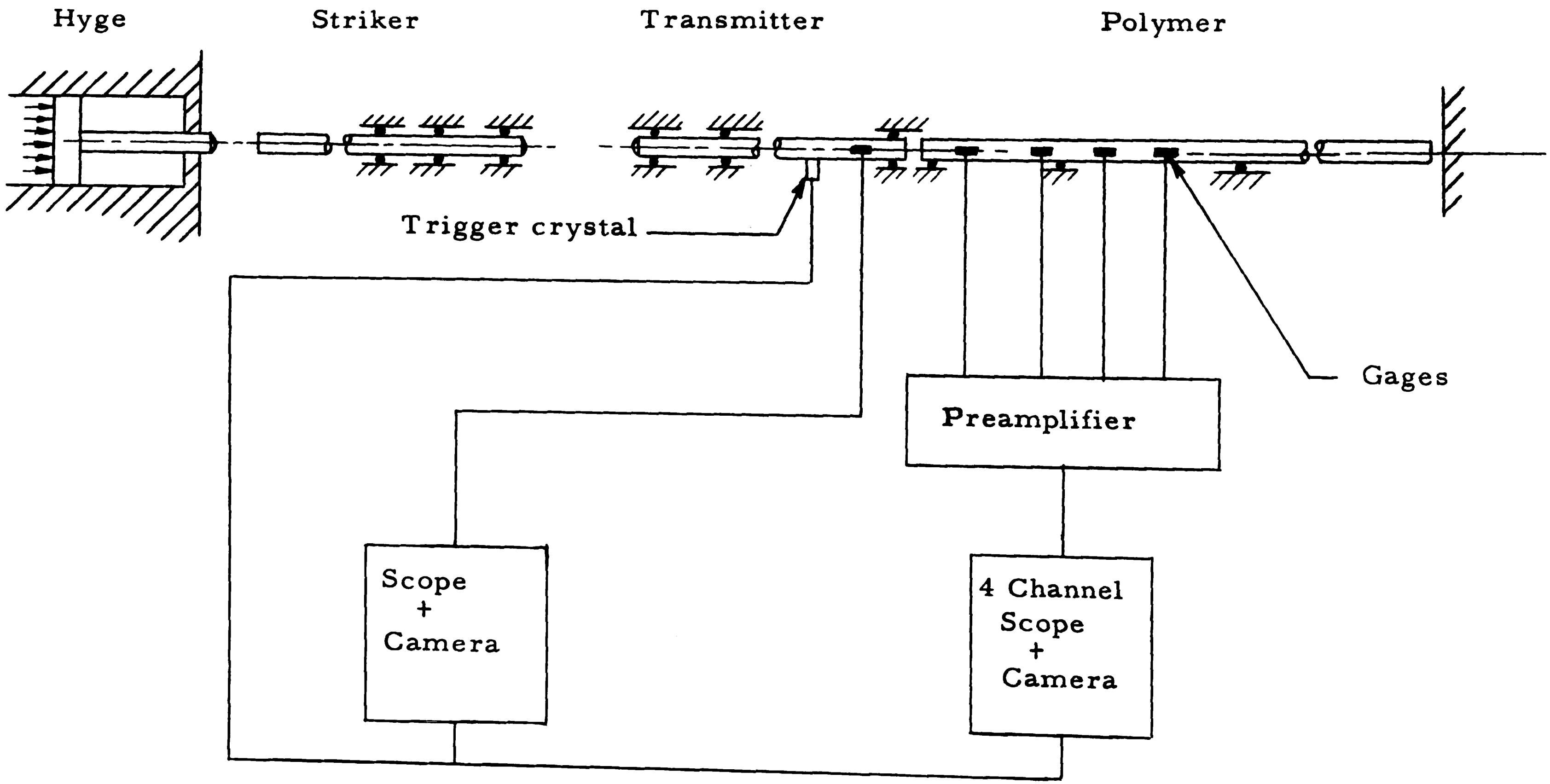

Figure 2. Impact Apparatus

in lubricated pillow blocks on an impacting frame about 22 feet long. A photograph of the apparatus is given in Figure 3.

When the accelerating device is triggered, the striker bar is pushed and accelerated down the impacting frame. Before the striker bar impacts the transmitter bar it leaves the pusher and moves as a free-free bar in the pillow blocks. After traveling a total of 18 inches the striker hits the transmitter bar which in turn moves 0.012 inches into contact with the polymer specimen. The small movement of the transmitter bar obviates the need for elaborate wiring installation in connection with instrumentation mounted on this bar. A photograph showing the polymer-transmitter bar interface is given in Figure 4.

When the striker bar impacts the transmitter bar a compressive wave moves out from the interface at a velocity equal to $\sqrt{E/\rho}$ relative to each bar. This wave travels down the transmitter bar until it reaches the free end, the end slightly separated from the polymer. At this point it is reflected as a tensile wave and now moves toward the striker end. The tensile stress and compressive stress in the incident and reflected wave add algebraically yielding zero stress in the section of the transmitter bar in the rear of the advancing tensile wave. It can be shown that the particle velocity in the compressed section of the transmitter bar is one-half the striker velocity while the particle velocity behind the advancing tensile wave is equal to the striker velocity. When the reflected pulse reaches the striker bar-transmitter bar interface, the bars, being the same length and density, exchange velocities and separate. This is discussed in Timoshenko and Goodier [1951].

The important point here is that after reflection of the compressive wave from the polymer end of the transmitter bar, the polymer end of the transmitter bar is stress free and moving at a constant velocity when it impacts the polymer rod. Now a new compressive pulse moves out from the polymer-transmitter bar interface, the gap having been set to

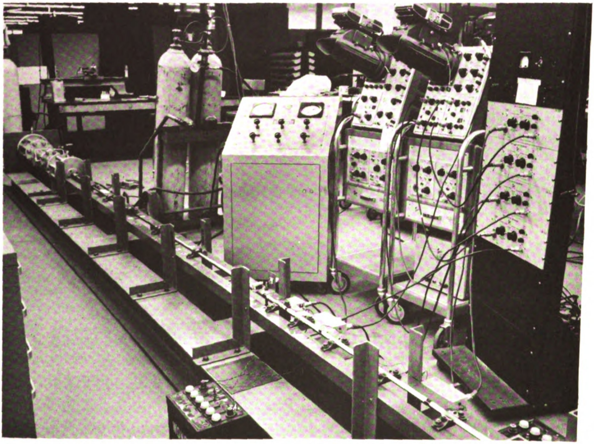

Figure 3. Photograph of the Impact Apparatus.

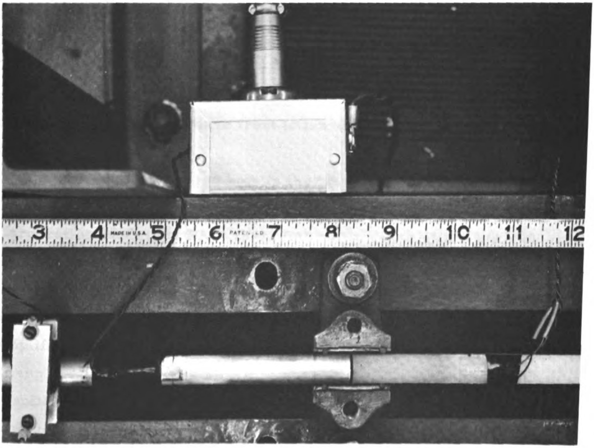

Figure 4. Photograph of the polymer-transmitter bar interface. The box on the top of the photograph contains the Wheatstone bridge. The trigger crystal is shown on the left.

allow this new compressive pulse to closely follow the reflected tensile wave front in the transmitter bar. Since the transmitter bar is stress free between these two wave fronts, a strain gage located near the polymer end of the transmitter bar can monitor this new compressive strain pulse as a function of time, which is recorded photographically from an oscilloscope trace. Since the pressure bar material is Hookean, from the strain record we can immediately calculate the stress, $\sigma(0, t)$. This stress pulse is, of course, the initial condition on the polymer bar. This is the procedure followed in this work. It should be noted that the duration in time of the boundary condition $\sigma(0, t)$ is equal to twice the time necessary for the wave front to travel the length of the transmitter bar.

Strain was monitored both in the polymer and magnesium bar with conventional strain gages. The gages used were Baldwin-Lima-Hamilton Corporation SR-4 type FAP-12-12 foil strain gages with a 1/4 inch gage length and were located as shown in Figure 2. To cancel bending stresses the gages were mounted on opposite sides of the rods and in opposite arms of a Wheatstone bridge. Output from the strain gage bridges was amplified and recorded photographically on oscilloscopes set for single sweep and triggered by a single ADP crystal. Various photographic results are shown in Figure 5. Detailed information on the electrical and mechanical system is given in Appendix III.

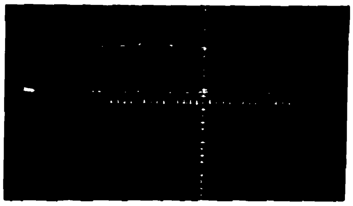

Strain versus time in the magnesium transmitter bar. From this photograph the boundary condition, $\sigma(0, t)$, on the polymer bar is determined. The scale is 50 microseconds per centimeter and 0.5 millivolts per centimeter.

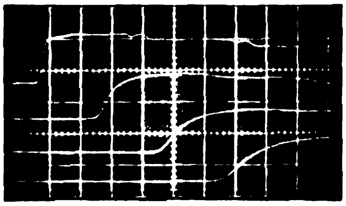

Strain versus time in the polymer bar. The upper trace is strain at x = 2 inches and lower trace at x = 32 inches. The scale is 150 microseconds per centimeter and about 10 millivolts per centimeter.

Figure 5. Typical oscilloscope records from the impact tests.

V. RESULTS

From Figure 5 it is seen that $\sigma(0, t)$ may be well represented for $t < 500$ microseconds by a Heaviside step function

$$\sigma(0, t) = \sigma_0 H(t) \tag{8}$$

where σ_0 is the amplitude of the square wave. It may be shown that this condition implies a constant velocity condition on the end of the bar, a condition frequently used in analytic work on the wave propagation problem. Using Equation (8) along with the linear damping relation, Equation (7), and the curve for phase velocity, Figure 1, Equation (5) may be evaluated numerically to yield the strain, $\epsilon(x, t)$, at each position on the polymer bar. The results of this calculation are plotted against the experimental results in Figures 6A, B, C, and D. Details of the numerical work are given in Appendix IV.

In comparing the results of the calculated strain to the experimentally measured strain, it was found that the magnitude of the curves differed by a factor of approximately two. Further investigation showed that the cement holding the gage to the polymer and the paper on which the gage is mounted actually had a restraining effect in the vicinity of the gage. The output of the gages was actually less than the strain present in the polymer. Constant strain rate compression tests performed on samples cut from the polymer rods with gages attached showed that the error was approximately independent of strain rate and constant for a large range of strains. This permitted a correction factor to be determined for the gage readings on the polymer bar. The details of these tests are given in Appendix V. The corrected values for the experimental strains are plotted in Figures 6A, B, C, and D and compared with the strains predicted by the calculation, using the end condition of Equation (8). In Figure 6, to better show the shape and amplitude correspondence of the computed and experimental waves, the curves have been shifted in time to put their initial arrival time, at each gage station, into agreement.

An attempt was also made to correlate the uncorrected strain measurements by taking the measured strain at $x = 2$ inches as an end condition to calculate the strain at the other stations. These uncorrected strains are shown in Figure 7 and are compared with the uncorrected experimental values. It is seen that the strain at $x = 2$ inches may be approximated by a step function (shown in the dotted lines), and to facilitate the calculation this approximation was used to predict the strain at $x = 12$, 22, and 32 inches. The agreement between calculated and experimental wave shape is excellent, however, the calculated curves are somewhat shifted in time.

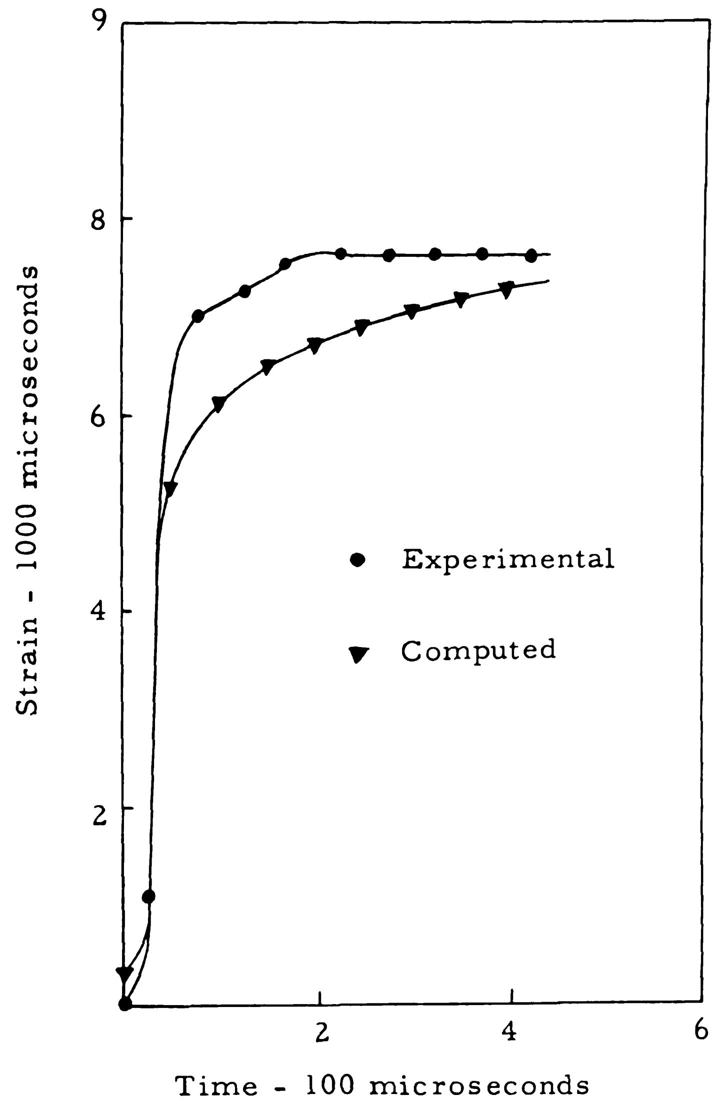

Figure 6A. Comparison of measured strain and computed strain at x = 2 inches. The curves have been shifted in time to compare shape and amplitude.

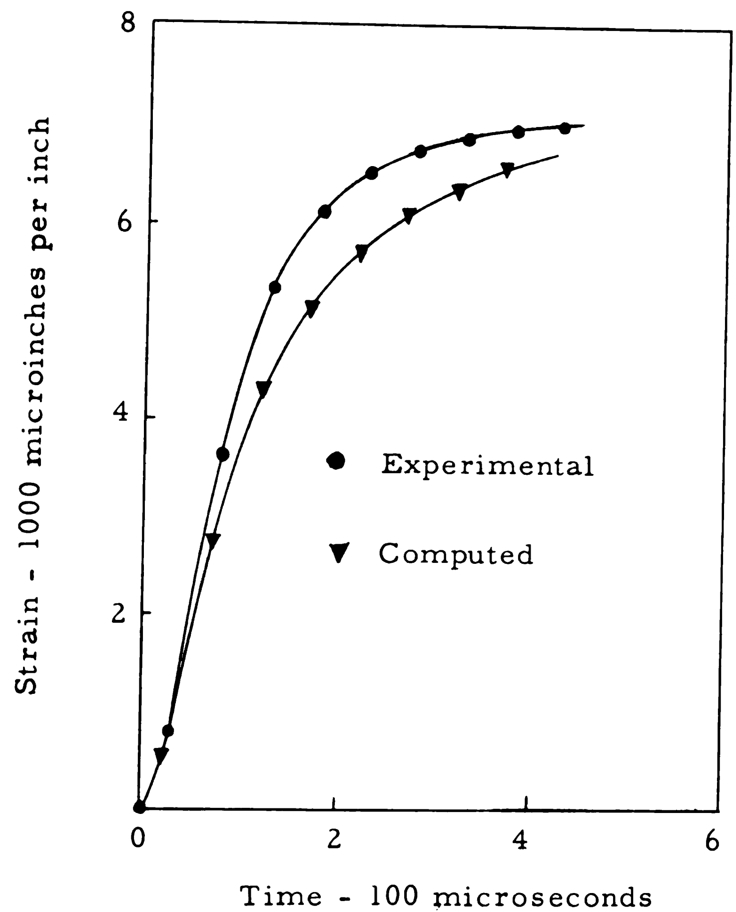

Figure 6B. Comparison of measured strain and computed strain at x = 12 inches. The curves have been shifted in time to compare shape and amplitude.

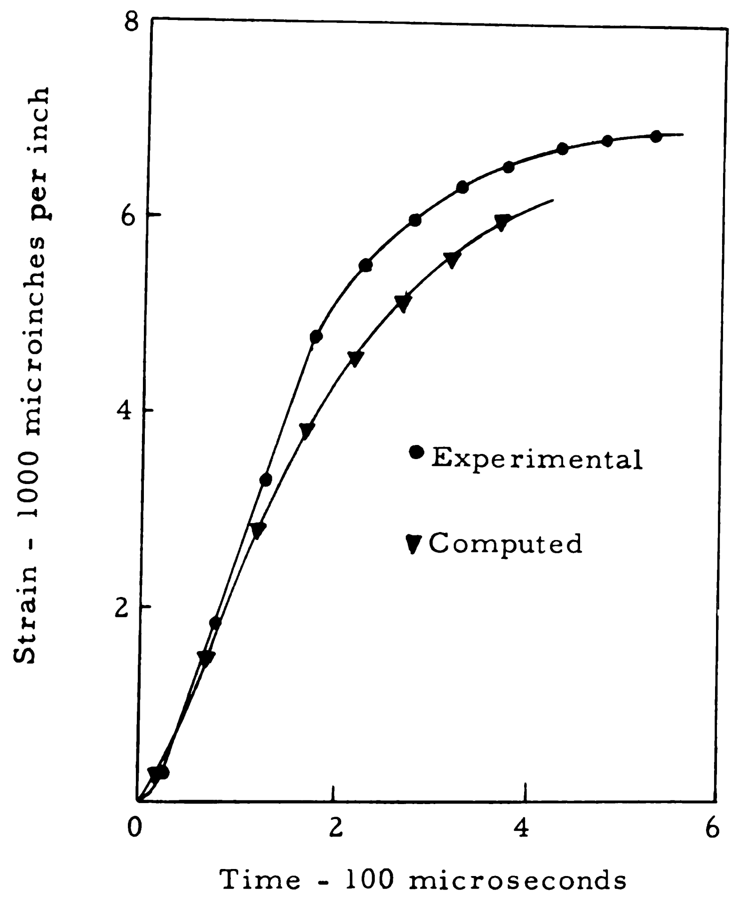

Figure 6C. Comparison of measured strain and computed strain at x = 22 inches. The curves have been shifted in time to compare shape and amplitude.

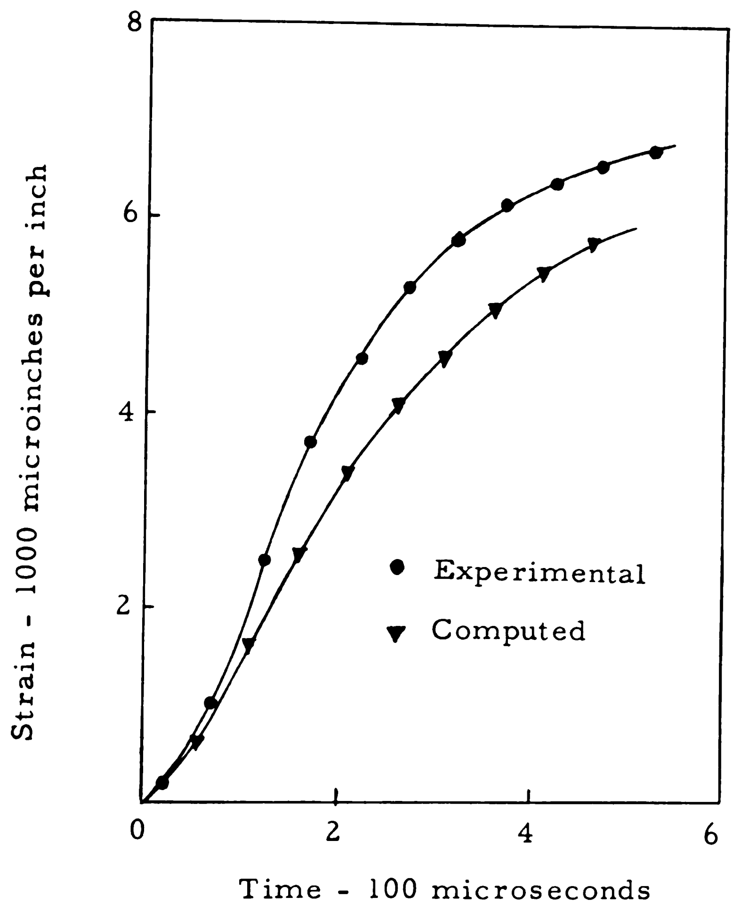

Figure 6D. Comparison of measured strain and computed strain at x = 32 inches. The curves have been shifted in time to compare shape and amplitude.

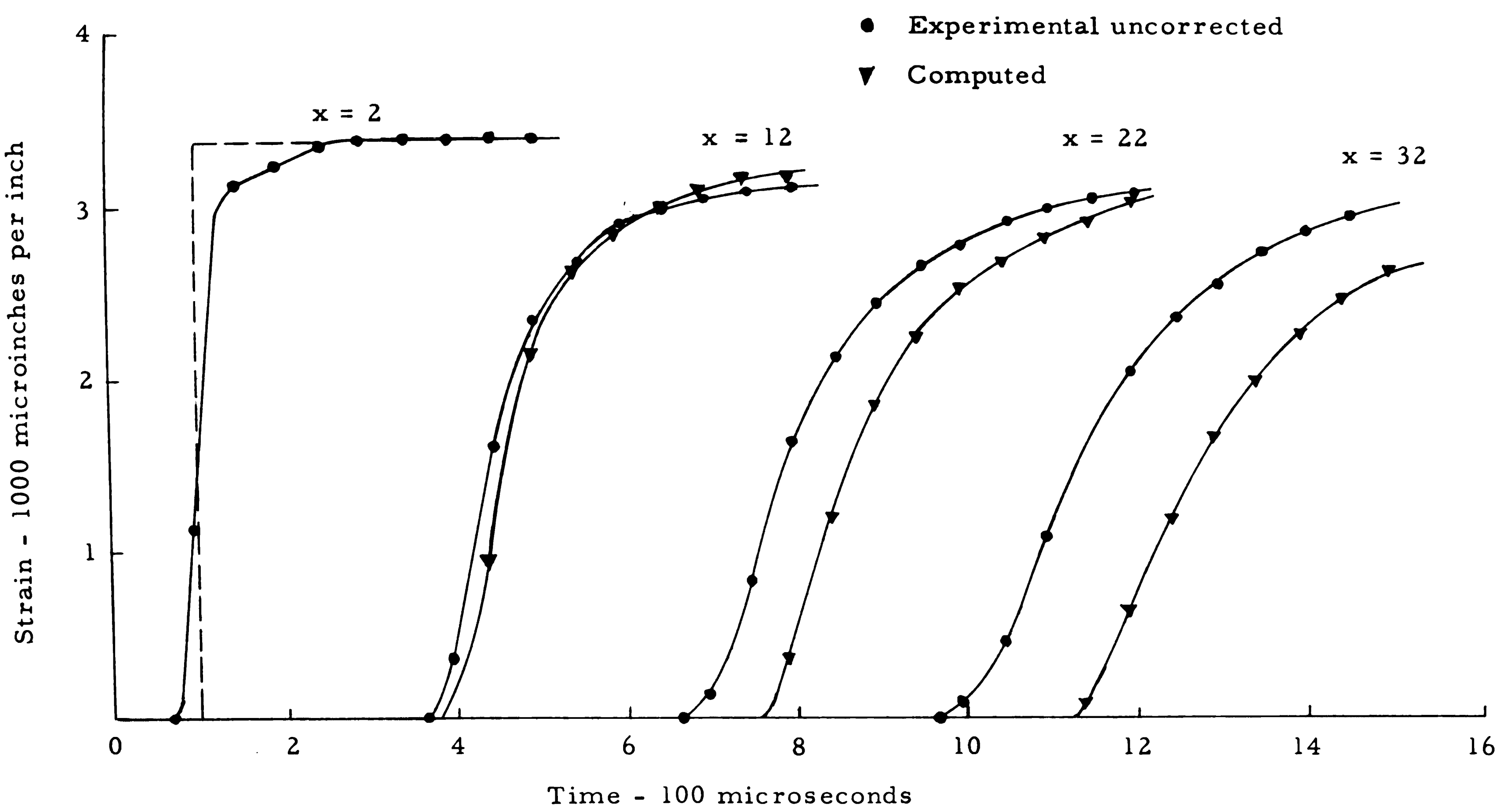

Figure 7. Comparison of measured strain and strain computed using the measured strain at x = 2 inches as a boundary condition.

VI. DISCUSSION OF RESULTS

It is obvious from Figure 7 that the calculated pulse is moving more slowly down the bar than the actual pulse. Since the agreement in amplitude and pulse shape is excellent, the disagreement between the two curves would seem to be in the phase velocity used in evaluating the integrals for the strain. It is thought the time difference might be eliminated by uniformly increasing the values of the phase velocity curve, Figure 1. A different shape of the phase velocity curve would destroy agreement in pulse shapes which is already quite good.

In particular, the high frequency components of the pulse are moving the fastest and hence are first to arrive at any given gage station on the polymer rod. It is seen from Figure 7 that these frequency components are moving at a velocity of about 32,800 inches per second while the maximum velocity given from the fiber tests is only 29,600 inches per second. The high frequency velocity read from Figure 7 for the computed curve is about equal to 29,600 inches per second as would be expected. Lee and Kanter [1953] showed that for a Maxwell model the head of the pulse is propagated at the maximum phase velocity of the solid. For comparison purposes it is to be noted that Hillier [1949], on a similar polyethylene, obtained an upper value of phase velocity of 37,800 inches per second.

Kolsky [1956] noticed a similar time discrepancy in comparing his observed pulse and calculated pulse. To obtain good correspondence between experimental and calculated pulse shapes, he found it was necessary to compare the experimental pulse at $x = 60$ cm. with the computed pulse at $x = 70$ cm. The results are shown in Figure 8.

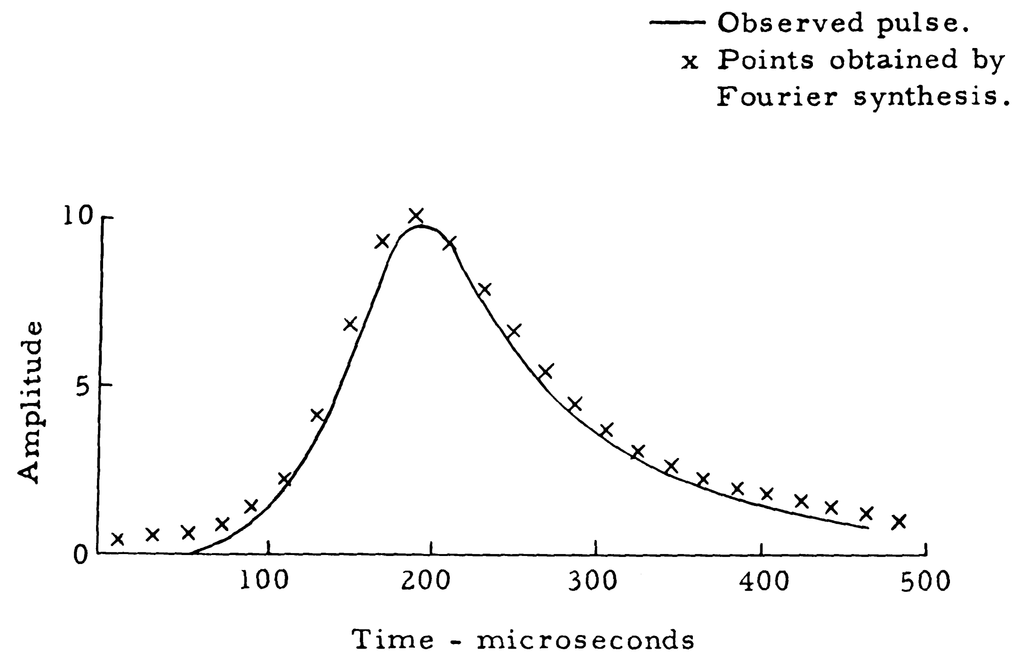

Figure 8. Comparison between observed pulse for 60 cm rod and curve calculated for 70 cm by Kolsky [1956].

Kolsky attributed the discrepancy to the initial geometric dispersion associated with an extremely short pulse and the inadequacy of representing the initial pulse as delta function. It is interesting to note here that Kolsky's results as shown in Figure 8 may be roughly interpreted to mean that the computed pulse is traveling too slowly. Geometric dispersion effects in an elastic bar would cause the high frequency components to travel more slowly than calculated by the elementary one-dimensional theory. Actual comparison of Kolsky's work and this work is difficult since Kolsky does not give a zero time reference.

The discrepancy in the computed and experimental velocities mentioned above may be due to orientation effects on the long polymer molecules during the extrusion process of the fibers, assuming the theory is correct. Hillier and Kolsky [1949] have shown that the complex modulus rises rapidly with increased orientation and hence the velocity does also.

Although care was taken in the extrusion so that little drawing occurred, it would seem difficult to maintain identical directional properties when extruding different diameter rods and fibers of diameter ratio of about 20 as was the case here. The results would have more significance if the material properties were measured on the rods to be impacted as done on lead by Bodner and Kolsky [1958].

It was found that the computed curves of Figure 6 (stress boundary condition) were actually shifted in time by the same amount as in Figure 7. However, since in Figure 6 it was a comparison of shape and amplitude which was desired, the computed curves have been shifted to put the initial arrival time into correspondence with initial arrival time of the experimental curves at each gage station. It is noted that if a multiplicative factor were applied to either set of curves of Figure 6, the amplitude and pulse shape would be in excellent agreement at all gage stations.

It should also be pointed out that while Bell [1960] found a measurable amount of the pulse exceeding the bar velocity, $\sqrt{E/\rho}$, in his elastic bar at five diameters from the end, in the polymer bar there seemed to be no such effect. It is difficult to draw conclusions from one such measurement (gage at $x = 2$ inches) but perhaps the problem is interesting enough to be investigated in more detail.

There is a question which arises in the assumption that the initial stress condition as measured in the strain gage at 3 inches from the end of the magnesium transmitter bar actually is an accurate measure of the stress on the end of the polymer bar. The elementary theory predicts the instantaneous formation of a step strain pulse which moves along the elastic magnesium bar at the bar velocity $\sqrt{E/\rho}$. Actually it takes a finite amount of time for this dilatational wave front to fully develop as Bell [1960] has shown. Using a 1/4 inch diameter striker bar he centrally impacted a two inch diameter bar and has shown the main detail of the pulse was formed by between three and five diameters.

With this type of central impact it would seem that due to the spherical nature of the wave in the first few diameters, the development of this wave front would take longer than for the case of impacting rods of the same diameter. Hence it is felt here that the wave monitored at $x = 3$ inches in the magnesium bar actually represents the developed shape of the boundary condition on the polymer bar. The development of the wave front in the first few diameters of a viscoelastic bar has not yet been investigated.

A more serious question is the applicability of SR-4 strain gages on polymers of very low elastic modulus. The test results given in Appendix V have shown decidedly different performance of strain gages mounted on polyethylene than performance in the usual metal application. A correction factor is required which appears to be relatively independent of strain and strain rate. Since the computed and experimental curves appear in good agreement at the 22 inch and 32 inch positions down the bar, it is thought that the restraining effect on the polymer of the cement-paper gage combination is a local effect and has little effect on the main part of the strain wave.

Little material appears in the literature on the application of SR-4 strain gages on low modulus polymers. SR-4 gages bonded to polymethyl methacrylate are discussed in a recent paper by Johnson and Homewood [1959]. Dietz and Campbell [1947] have made a rather thorough investigation of the effects of a number of cements available at that time on polymethyl methacrylate and polystyrene. The conclusions indicated the paper backing of the gage may introduce errors in low modulus materials.

It is known that a number of people are working on methods for monitoring strains in low modulus polymers because of the application to stress analysis in solid rocket propellents which are viscoelastic in nature. Much of the work is proprietary in nature and does not appear in the literature. However, two obvious methods of solving the problem are defraction grating techniques or perhaps use of an extensometer and some associated photoelectric circuitry. Radial capacitive gages would introduce another variable in the form of a viscoelastic Poisson effect. These methods would involve added complications and further investigation of the SR-4 gage in this application would be profitable.

A number of analytical solutions to the impact problem have been given for particular materials, e.g. Voigt, Maxwell, standard linear solid, etc. It would be interesting to see how well these solutions would agree with the experimental results obtained in the present work. The various model parameters could be obtained from a method such as given by Bland [1960] using data presented in Appendix II on the complex compliance for polyethylene. Because of the limited frequency range of the complex compliance necessary here for the Fourier analysis, it is thought a good fit might be obtained over the significant portions of the frequency spectrum. Kolsky [1949] has used this fact in a different problem to predict stress strain behavior of polyethylene even when the material does not behave as the model over large frequency ranges.

In conclusion, the work presented here seems to confirm the accuracy of the theory of impact of the linear polymer polyethylene for small strains pulses in the time range of 500 microseconds and represents the primary contribution of the work. A number of associated problems arising in the work have been presented which, it is hoped, will motivate further investigation.

BIBLIOGRAPHY

Alfrey, T. Mechanical Behavior of High Polymers, Interscience Publishers, Inc., New York, 1948.

Ballou, J. W. and Smith, J. C. "Dynamic Measurements of Polymer Physical Properties," J. Appl. Phys., vol. 20, 1949, pp. 493-502.

Bell, J. F. "The Initial Development of an Elastic Strain Pulse Propagating in a Semi-Infinite Bar," Technical Report No. 6, The John Hopkins University, 1960.

Bergen, J. T. Viscoelasticity, Phenomenological Aspects, Academic Press, New York, 1960.

Berry, D. S. and Hunter, S. C. "The Propagation of Dynamic Stresses in Visco-Elastic Rods," J. Mech. Phys. Solids, vol. 4, 1956, p. 72.

Bland, D. R. The Theory of Linear Viscoelasticity, Pergamon Press, New York, 1960.

Bodner, S. R. and Kolsky, H. "Stress Wave Propagation in Lead," Proc. 3rd U. S. Nat. Cong. Appl. Mech., A.S.M.E., New York, 1958, p. 495.

Charles, H. "On the Wave Equation in a Hereditary Field," Bull. Soc. roy. Sci. Liege, vol. 20, no. 3, 1951, pp. 195-198 (in French).

Chree, C. "The Equations of an Isotropic Elastic Solid in Polar and Cylindrical Coordinates, Their Solution and Application," Trans. Camb. Phil. Soc., vol. 14, 1889, p. 250.

Davies, R. M. "A Critical Study of the Hopkinson Pressure Bar," Phil. Trans. roy Soc. (A), vol. 240, 1948, pp. 375-457.

Dietz, A. G. H. and Campbell, W. H. "Bonded-wire Resistance Strain Gage Techniques for Polymethyl Methacrylate Plastics," Proc. Soc. Exper. Stress. Anal., vol. V, no. 1, 1947, pp. 59-62.

Eubanks, R. A., Muster, D., and Volterra, E. "On the Attenuation of a Sinusoidal Pulse in a Cylindrical Specimen Held Between Elastic Bars," Proc. 2nd U.S. Nat. Cong. Appl. Mech., A.S.M.E., New York, 1954, pp. 193-197.

Glauz, R. D. and Lee, E. H. "Transient Wave Analysis in a Linear Time-dependent Material," J. Appl. Phys., vol. 25, 1954, pp. 947-953.

Gross, B. Mathematical Structure of the Theories of Viscoelasticity, Herman et Cie, Paris, 1953.

Habib, E. T. "A Method of Making High-Speed Compression Tests on Small Copper Cylinders," J. Appl. Mech., vol. 15, no. 3, 1948, p. 248.

Hillier, K. W. "The Measurement of Some Dynamic Constants and Its Application to the Study of High Polymers," Proc. Phys. Soc., vol. 62, 1949, pp. 701-713.

_________. "The Measurement of Dynamic Elastic Properties," Progress in Solid Mechanics, edited by Sneddon, I. N. and Hill, R., vol. 2, North-Holland Pub. Co., Amsterdam, 1960, pp. 201-242.

_________ and Kolsky, H. "An Investigation of the Dynamic Elastic Properties of Some High Polymers," Proc. Phys. Soc., vol. 62, 1949, pp. 111-121.

Hunter, S. C. "Viscoelastic Waves," Progress in Solid Mechanics, edited by Sneddon, I. N. and Hill, R., vol. 1, North-Holland Pub. Co., Amsterdam, 1960, pp. 3-57.

Johnson, A. E., Jr. and Homewood, R. H. "Stress and Deformation Analysis from Reduced-scale Plastic-model Testing," Proc. Soc. Exper. Stress Anal., vol. 18, no. 2, 1959, pp. 81-90.

Kolsky, H. "An Investigation of the Mechanical Properties of Materials of Very High Rates of Loading," Proc. Phys. Soc. London (B), vol. 62, 1949, pp. 676-700.

_________. Stress Waves in Solids, Oxford University Press, Oxford, 1953.

Kolsky, H. "The Propagation of Stress Pulses in Viscoelastic Solids," Phil. Mag., vol. 8, no. 1, 1956, p. 693.

________. "The Propagation of Stress Waves in Viscoelastic Solids," Appl. Mech. Rev., vol. 11, no. 9, Sept. 1958, pp. 465-468.

________. "The Mechanical Testing of High Polymers," Prog. in Non-Destructive Testing, vol. 2, 1959, pp. 29-59.

________. "Viscoelastic Waves," International Symposium on Stress Wave Propagation in Materials, edited by Norman Davids, Interscience Publishers, Inc., New York, 1960, pp. 59-90.

Kunz, K. S. Numerical Analysis, McGraw Hill, New York, 1957.

Leaderman, H. Elastic and Creep Properties of Filamentous Materials and Other High Polymers, The Textile Foundation, Washington, D.C., 1943.

Lee, E. H. and Kanter, I. "Wave Propagation in Finite Rods of Viscoelastic Material," J. Appl. Phys., vol. 24, 1953, pp. 1115-1122.

Love, A. E. H. A Treatise on the Mathematical Theory of Elasticity, 4th Ed., Dover Publications, New York, 1926, pp. 287.

Malvern, L. E. "Plastic Wave Propagation in a Bar of Material Exhibiting a Strain Rate Effect," Quart. Appl. Math., vol. 8, 1951, pp. 405-411.

Morrison, J. A. "Wave Propagation in Rods of Voigt Materials and Viscoelastic Materials with Three-Parameter Models," Quart. Appl. Math., vol. 14, 1956, pp. 153-169.

Pochhammer, L. "Uber Fortpflanzungsgeschwindigkeiten Kleiner Schwingungen in einem Unbegrenzten Isotropen Kreiszylinder," J. Reine Angew. Math. (Crelle), vol. 81, 1876, p. 324.

Ricker, N. "Further Development in the Wavelet Theory of Seismogram Structure," Bull. Seism. Soc. Amer., vol. 33, 1943, pp. 197-228.

Sips, R. "Propagation Phenomena in Elastic-Viscous Media," J. Polymer. Sci., vol. 6, no. 3, 1951, pp. 191-205.

Sips, R. "General Theory of Deformation in Viscoelastic Substances," J. Polymer Sci., vol. VII, no. 2/3, 1951, pp. 285-293.

Thompson, J. H. C. "On the Theory of Viscoelasticity: a Thermodynamical Treatment of Viscoelastic Solids," Phil. Trans. roy. Soc. (A), vol. 231, 1933, pp. 339-407.

Timoshenko, S. and Goodier, J. N. Theory of Elasticity, 2nd Ed., McGraw-Hill Book Co., New York, 1951, p. 444.

Tsien, H. S. "A Generalization of Alfrey's Theorem for Viscoelastic Media," Quart. Appl. Math., vol. 8, 1950, p. 104.

Weber, W. "Ueber die Elasticitat der Seidenfäden," Pogg. Ann. Physik (2), vol. 4, 1835, p. 247.

Zverev, I. N. "The Propagation of a Disturbance in a Viscoelastic and Viscoplastic Bar," Prikl. Mat. Mekh., vol. 14, 1950, pp. 295-302 (in Russian). Translation A11-T12/16, Brown Univ.

APPENDICES

APPENDIX I

THEORY

The equations necessary to describe uniaxial wave propagation in a viscoelastic rod are the stress strain relationship, the equation of motion, the strain displacement relationship, and the associated boundary and initial conditions. Two of these equations are identical to those of elasticity theory and the only problem arises in a choice of a suitable viscoelastic stress strain relationship.

A number of investigators have analyzed wave propagation problems by idealizing the material to yield a usable stress strain relationship. Behavior corresponding to Maxwell, Voigt or combination models is assumed which gives an nth order linear differential equation relating stress and its time derivatives to strain and its time derivatives. Unfortunately, not many real materials behave as these simple idealizations. It is necessary in many cases to take a considerable number of elements to get significant correspondence over a wide frequency range. This in general leads to mathematical difficulties.

A more general approach to a stress strain relationship is achieved by use of the Boltzmann superposition integral. The linear superposition concept is used to generalize the results of a uniaxial relaxation test to a strain varying with time. The following argument is given in more detail in Leaderman [1943].

Consider a uniaxial relaxation test where at time $t = 0$, a thin rod of viscoelastic material is subjected to a step strain, $\epsilon = \epsilon_0 H(t)$, where $H(t)$ is the Heaviside unit function. The resulting stress, $\sigma(t)$, is given by

$$\begin{aligned} \sigma(t) &= E_D \epsilon_0 (1 - \phi(t)) \qquad & t \geq 0 \\ &= 0 & t < 0 \end{aligned} \tag{11}$$

$\phi(t)$ is called the relaxation function, a positive, monotonic function increasing with time and independent of the stress and strain amplitude. E_D is the dynamic Young's modulus of the material. The relaxation function is usually measured from an uniaxial relaxation test although other methods are available.

Equation (11) may be generalized by use of the superposition integral to apply to a more general strain loading by the integral equation

$$\sigma(t) = E_D \left\{ \epsilon(t) - \int_{-\infty}^{t} \frac{d\epsilon(\tau)}{d\tau} \phi(t-\tau)d\tau \right\} \tag{12}$$

which is taken here to be the fundamental constitutive equation relating stress and strain. Gross [1953] has shown it is equally acceptable to define a creep function through a simple creep test and arrive at a similar relationship. He has shown that the creep and relaxation functions are not independent and may be related by a Laplace transform.

The stress-strain relation together with the equation of motion

$$\frac{\partial \sigma}{\partial x} = \rho \frac{\partial^2 u}{\partial t^2} \tag{13}$$

and the strain-displacement relationship

$$\epsilon = \frac{\partial u}{\partial x} \tag{14}$$

together with the boundary and initial conditions are the defining equations of the problem.

It is convenient to solve these equations by a Fourier method. The solution given below essentially follows the method given by Hunter [1960]. The Fourier integral theorem may be written

$$\pi f(x,t) = \int_0^{\infty} d\omega \int_{-\infty}^{\infty} f(x,\xi) \cos[\omega(t-\xi)]d\xi \tag{15}$$

from which we may define the one-sided Fourier transform

$$\bar{f}(x, \omega) = \int_0^\infty f(x, t) e^{-i\omega t}\, dt$$
$$\pi f(x, t) = R\left\{ \int_0^\infty \bar{f}(x, \omega) e^{i\omega t} d\omega \right\} \tag{16}$$

provided $f(x, t) = 0$ for $t \leq 0$, $f(x, t)$ is sectionally continuous and the integral

$$\int_0^\infty |f(x, t)|\, dt \tag{17}$$

converges uniformly on x. These conditions are all satisfied for the case of the pulse considered here but not satisfied for steady-state vibrations.

Applying the transform to the stress strain relation and making use of the convolution theorem we have

$$\bar{\sigma}(\omega) = E_D\, [1 + i\omega\bar{\phi}(\omega)]\, \bar{\epsilon}(\omega) \tag{18}$$

where the bars indicate the transformed variables. This transformed stress strain relation may be rewritten for simplicity as

$$\bar{\sigma}(\omega) = E_0(i\omega)\, \bar{\epsilon}(\omega) \tag{19}$$

where $E_0(i\omega)$ is defined from equation (18).

Hunter [1960] has shown how the convergence problem arising in a direct Fourier transform of a sinusoidally varing strain may be avoided. He applies a Laplace transform to the constitutive Equation (12) where now $\epsilon = \bar{\epsilon}(\omega) e^{i\omega t}$ is a periodic strain initiated at time $t = 0$. The resulting equation is inverted by use of the complex inversion integral. The result, after initial transients die out, is

$$\bar{\sigma}(\omega) = E(i\omega)\,\bar{\epsilon}(\omega) \tag{20}$$

where $\sigma = \bar{\sigma}(\omega)e^{i\omega t}$. This equation is identical to Equation (19) if $E_0(i\omega) = E(i\omega)$.

$E(i\omega)$ is a complex function of the real variable ω and relates the amplitude and phase of the periodic stress and strain. $E(i\omega)$ is known as the complex modulus and completely defines the material properties of a viscoelastic material. It is conveniently obtained by steady state vibration tests as is later shown. This, in fact, is the reason the Fourier transform is used here rather than the Laplace transform.

The one-sided Fourier transform of Equations (13) and (14) are respectively for the initially dead bar

$$\frac{\partial \bar{\sigma}(x, \omega)}{\partial x} = \rho\ (i\omega)^2 \bar{u}(x, \omega) \tag{21}$$

$$\bar{\epsilon}(x, \omega) = \frac{\partial \bar{u}(x, \omega)}{\partial x} \tag{22}$$

where the bar again indicates a transformed variable. Note with Equation (20), Equations (21) and (22) form a set similar to the elastic wave problem. It is this similarity which forms the basis of the elastic-viscoelastic correspondence principle previously referred to.

Combining these two equations and the transformed stress-strain relationship yields

$$\left\{ \frac{\partial^2}{\partial x^2} - \lambda^2(i\omega) \right\} \bar{\epsilon}(x, \omega) = 0 \tag{23}$$

where

$$\left.\begin{aligned} \lambda^2(i\omega) &= \frac{(i\omega)^2 \rho}{E(i\omega)} \\ \lambda &= \lambda_1 + i\lambda_2. \end{aligned}\right\} \tag{24}$$

Solving Equation (23) gives

$$\bar{\epsilon}(x, \omega) = C(\omega)e^{-\lambda x} + D(\omega)e^{\lambda x} \tag{25}$$

where C and D are found from the boundary conditions.

For the semi-infinite bar we have the condition

$$\lim_{x \to \infty} \sigma(x, t) = 0$$

which transforms to

$$\lim_{x \to \infty} \bar{\sigma}(x, \omega) = E(i\omega) \lim_{x \to \infty} \bar{\epsilon}(x, \omega) = 0 \tag{26}$$

and yields $D(\omega) = 0$. At the end $x = 0$, the boundary condition is one of stress as a function of time and Equation (25) becomes

$$\bar{\epsilon}(x, \omega) = \bar{\epsilon}(o, \omega)e^{-\lambda x} = \frac{\bar{\sigma}(o, \omega)}{E(i\omega)} e^{-\lambda x} . \tag{27}$$

This equation is inverted by the inverse one-sided Fourier transform to give the solution

$$\pi\epsilon(x, t) = R\left\{\int_0^\infty \frac{\bar{\sigma}(o,\omega)}{E(i\omega)} e^{-\lambda x + i\omega t}\right\}d\omega \tag{28}$$

And since

$$\bar{\sigma}(o, \omega) = \int_0^\infty \sigma(o, t)e^{-i\omega t}\, dt = \int_0^\infty \sigma(o, t)\cos\omega t dt - i\int_0^\infty \sigma(o, t)\sin\omega t dt, \tag{29}$$

it is convenient to define

$$\bar{\sigma}(o, \omega) = \bar{\sigma}_R(\omega) - i\, \bar{\sigma}_I(\omega) \tag{30}$$

where

$$\bar{\sigma}_R(\omega) = \int_0^\infty \sigma(o,t)\cos\omega t dt \qquad \bar{\sigma}_I(\omega) = \int_0^\infty \sigma(o,t)\sin\omega t dt. \tag{31}$$

Replacing the complex modulus, $E(i\omega)$, by the complex compliance, $J(i\omega)$, where

$$J(i\omega) = \frac{1}{E(i\omega)} = J_R + iJ_I \tag{32}$$

and $\bar{\sigma}(o,\omega) = \bar{\sigma}_R(\omega) - i\bar{\sigma}_I(\omega)$, Equation (28) becomes

$$\pi\epsilon(x,t) = R\left\{\int_0^\infty (J_R + iJ_I)(\bar{\sigma}_R - i\bar{\sigma}_I)e^{-\lambda_1 x}e^{i(\omega t - \lambda_2 x)}d\omega\right\}. \tag{33}$$

From Equation (33) it is seen that λ_1 corresponds to a frequency dependent damping coefficient which is usually denoted $\alpha(\omega)$. If λ_2 corresponds to the angular velocity ω divided by the phase velocity $c(\omega)$, the solution, Equation (33), could represent the case of a strain pulse moving down the bar. A Fourier analysis shows the pulse is composed of a distributed spectrum of frequencies each of which is propagated at a different velocity $c(\omega)$ and damped as a function of frequency and position down the bar. Hence the pulse will be dispersed and attenuated as it moves down the bar.

Substituting in Equation (33) for λ and taking the real part of the integral we finally have

$$\pi\epsilon(x,t) = \int_0^\infty \exp[-\alpha(\omega)x]\ \left[A(\omega)\cos[\omega(t-\frac{x}{c(\omega)})] + B(\omega)\sin[\omega(t-\frac{x}{c(\omega)})]\right] d\omega$$

$$A(\omega) = J_R\bar{\sigma}_R + J_I\bar{\sigma}_I \qquad B(\omega) = J_R\bar{\sigma}_I - J_I\bar{\sigma}_R. \tag{34}$$

The complex compliance may be put in a more convenient form by use of Equation (24), (32) and the definition of λ as a complex function of $\alpha(\omega)$ and $c(\omega)$. This results in the relationships

$$J_R(\omega) = \frac{1}{\rho\ \bar{c}(\omega)^2}$$

$$J_I(\omega) = -\frac{2\alpha(\omega)}{\rho\ c(\omega)\omega} \tag{35}$$

where it has been assumed that $\alpha(\omega)$ is small compared to $\frac{\omega}{c}$. Equation (20) motivates a method for determining the complex modulus and compliance by experimentally measuring $c(\omega)$ and $\alpha(\omega)$ in a steady state vibration test.

If it is now assumed $\alpha(\omega)$ is proportional to the angular frequency ω by a factor of proportionality k_1, Equation (35) becomes

$$J_I(\omega) = -\frac{2\,k_1}{\rho\, c(\omega)} \tag{36}$$

from which $A(\omega)$ and $B(\omega)$ of Equation (34) become

$$\begin{aligned} A(\omega) &= \frac{1}{\rho\, c^2}\,(\bar{\sigma}_R - 2k_1 c\,\bar{\sigma}_I\;) \\ B(\omega) &= \frac{1}{\rho\, c^2}\,(\bar{\sigma}_I + 2k_1 c\,\bar{\sigma}_R). \end{aligned} \tag{37}$$

If the phase velocity $c(\omega)$ and damping $\alpha(\omega)$ are known for a given material and the boundary condition, $\sigma(o,t)$, on the end of the semi-infinite bar is known, Equations (34) and (37) constitute the complete solution to the one-dimensional wave propagation problem.

Kolsky [1956] has considered the case when the boundary condition is given by a sharp impact which may be represented

$$\sigma(o,t) = A\;\delta(t) \tag{38}$$

where $\delta(t)$ is the Dirac delta function. Now if Equation (34) is derived in terms of stress only, it can be shown that

$$\pi\,\sigma(x,t) = \int_0^\infty \exp(-\alpha(\omega)x)\left\{\bar{\sigma}_R\cos[\omega(t-\frac{x}{c})] + \bar{\sigma}_I\sin[\omega(t-\frac{x}{c})]\right\}d\omega. \tag{39}$$

Using Equation (38) and the definitions of $\bar{\sigma}_R$ and $\bar{\sigma}_I$ it is easily shown that Equation (39) reduces to

$$\pi\,\sigma(x,t) = A\int_0^{\infty} \exp\,(-a(\omega)x)\cos[\omega(t - \frac{x}{c})]\,d\omega. \tag{40}$$

Kolsky has solved this equation by a series approximation and compared the results with experimental impact, using an explosive to create an approximation to the delta function.

For a boundary condition on strain, it is easily shown that Equation (27) reduces to Equation (6).

APPENDIX II

EXPERIMENTAL DETERMINATION OF THE COMPLEX COMPLIANCE

The complex compliance has been defined in terms of the material damping $\alpha(\omega)$ and the phase velocity $c(\omega)$ in Equation (35), which is repeated here for convenience

$$J = J_R + i\, J_I = \frac{1}{\rho\, c(\omega)^2} - i\,\frac{2\,\alpha(\omega)}{\rho\,\omega\; c(\omega)} \; . \tag{41}$$

Hence if the phase velocity and damping can be measured as a function of frequency, the stress strain relation, Equation (19), may be completely specified in the transformed space.

A number of experimental techniques are available for the measurement of the parameters; the method of measurement is largely determined by the relevant frequency range desired. A survey of experimental techniques in this area is given by Hillier [1961]. For this problem the nature of the damping term in the integral of Equation (34) suggests frequencies above some number may be neglected. It later will be shown that this upper limit is of the order of the audio spectrum and hence a method giving $\alpha(\omega)$ and $c(\omega)$ over the audio range was selected.

A convenient method for measuring these parameters over this frequency range is to apply a steady sinusoidal longitudinal displacement to one end of a long rod or fiber and physically measure the attenuation and velocity of the resulting traveling waves at a constant frequency. The theory is well discussed by Ballou and Smith [1949] and by Hillier and Kolsky [1949]. A thin string or fiber of the material to be tested is usually used because of lack of availability of high power sinusoidal drivers with adequate frequency response. The sensing device is some type of crystal in physical contact with the fiber and designed so that it might be moved accurately along the fiber. If the length of the fiber is long compared to the distance between the driver and crystal pick-up and the material has sufficient damping properties, the string may be considered semi-infinite and no waves are reflected from the terminated end. Reflections from the pick-up, however, must be included in the analysis.

The displacement at a distance x from the driver is given by

$$u_1 = ae^{-\alpha x} e^{i(\omega t - kx)} . \tag{42}$$

The wave reflected from the pick-up is

$$u_2 = -ame^{-\alpha(2\ell - x)} e^{i[\omega t - k(2\ell - x)]} \tag{43}$$

where ℓ is the distance between the pick-up and the driver and m is the reflection coefficient. From these equations it may be shown that the phase angle, θ, between the fiber displacement at the driver and that at the pick-up is given by

$$\tan\theta = \frac{1+me^{-2\alpha\ell}}{1-me^{-2\alpha\ell}} \tan k\ell . \tag{44}$$

If $m \ll 1$ and $\alpha\ell$ is large, we may take $\theta \doteq k\ell$ and hence the velocity may be determined. Equation (44) represents a straight line of slope k on which is superimposed an oscillation rapidly decaying with distance along the fiber. One such curve is given in Figure 9.

The ratio of the amplitude of the signal at the pickup, B, to that at the driver, A, may be shown to be

$$\frac{B}{A} = (1-m)e^{-\alpha\ell}[1 - 2\,me^{-2\alpha\ell}\cos 2k\ell + m^2e^{-4\alpha\ell}]^{-\frac{1}{2}} . \tag{45}$$

For materials of relatively high damping a plot of the logarithm of $\frac{B}{A}$

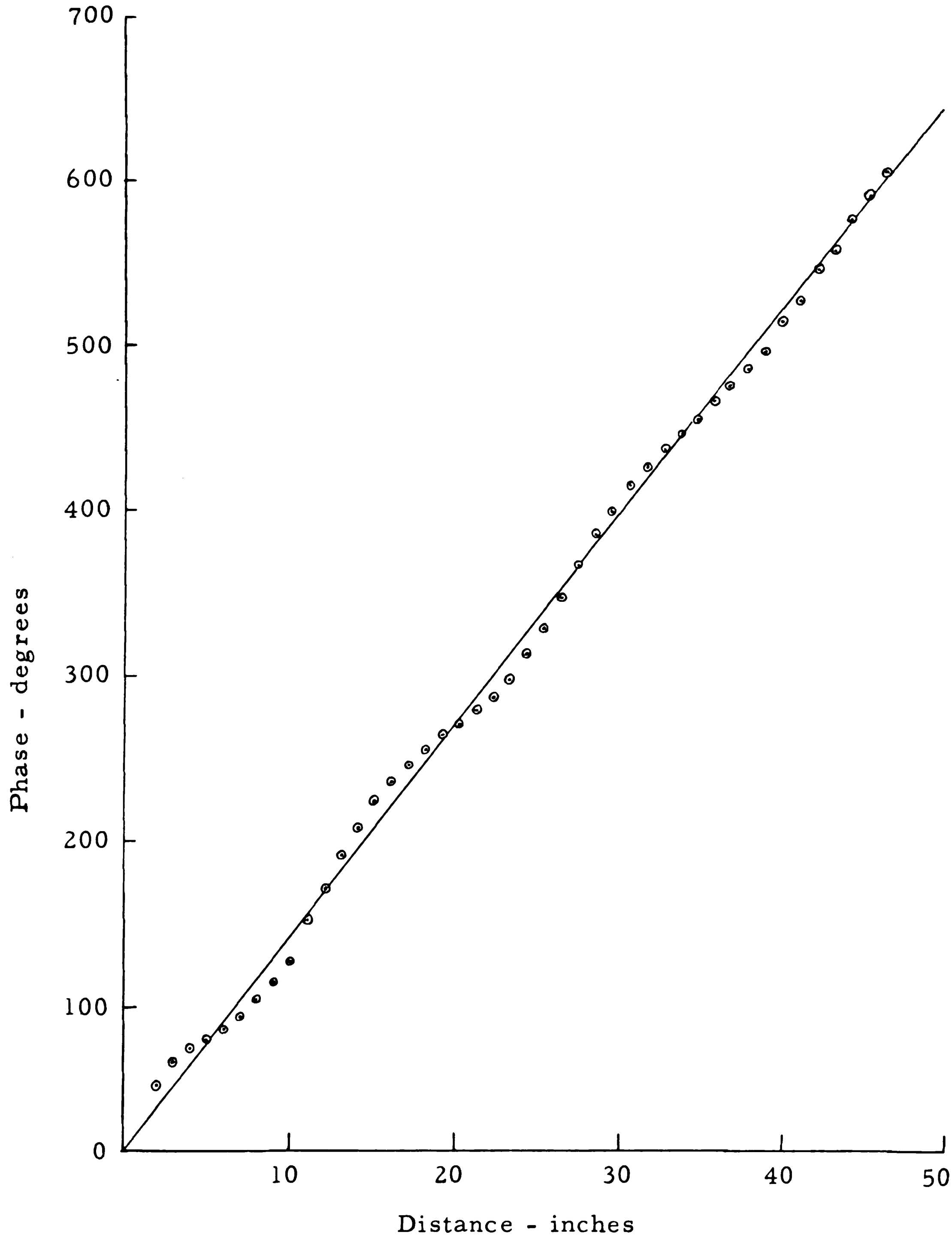

Figure 9. Fiber Test on Polyethylene at 900 cps and 75°F. The phase velocity, $c(\omega)$, may be obtained from the slope of this curve.

versus distance along the string gives α. A sample curve is given in Figure 10. For materials of smaller damping it becomes much more difficult experimentally to obtain information from Equation (45) than Equation (44). Ballou and Smith [1949] and Hillier and Kolsky [1949] both give methods which will allow measurement of α for cases of low damping. The material used in this work had high damping characteristics and α was obtained by a direct plot of the logarithm of the amplitude ratio against distance along the fiber.

Unoriented fibers of the same polyethylene as that used in the impact tests were obtained for the work here. Fiber diameter was 0.030 ± 0.001 inch; various lengths from 47 inches to 24 feet were used. In the extrusion of the fibers and the rods an effort was made to minimize any geometric effects due to the extrusion process. Since the diameters differ by a factor of about 20 it is difficult to keep identical molecular orientation, however, since both the fibers and rods were undrawn it was initially felt that this was not a serious problem.

The driver was a phonograph record cutter head, Audax Model RH-5. The response of this unit was $\pm$ 2 db from 1,000 to over 13,000 cps and adequate response (from 100 to 25,000 cps) for this application. Distortion is 1.2% at 1000 cps. A magnesium needle was drilled to accept the fiber and the needle mounted in the cutter head.

The pick-up used was a PZT ceramic, Electro-Voice, Model 21 phonograph cartridge with a rated output of 0.5 volts. The response of this unit is from 20 to 20,000 cps. The standard pick-up needle was removed from the needle arm and a small grooved polymethyl methacrylate contactor was designed and cemented to the arm. The cartridge was mounted so that the needle pointed vertically upward with the fiber positioned perpendicular to the needle arm and touching the grooved contactor.

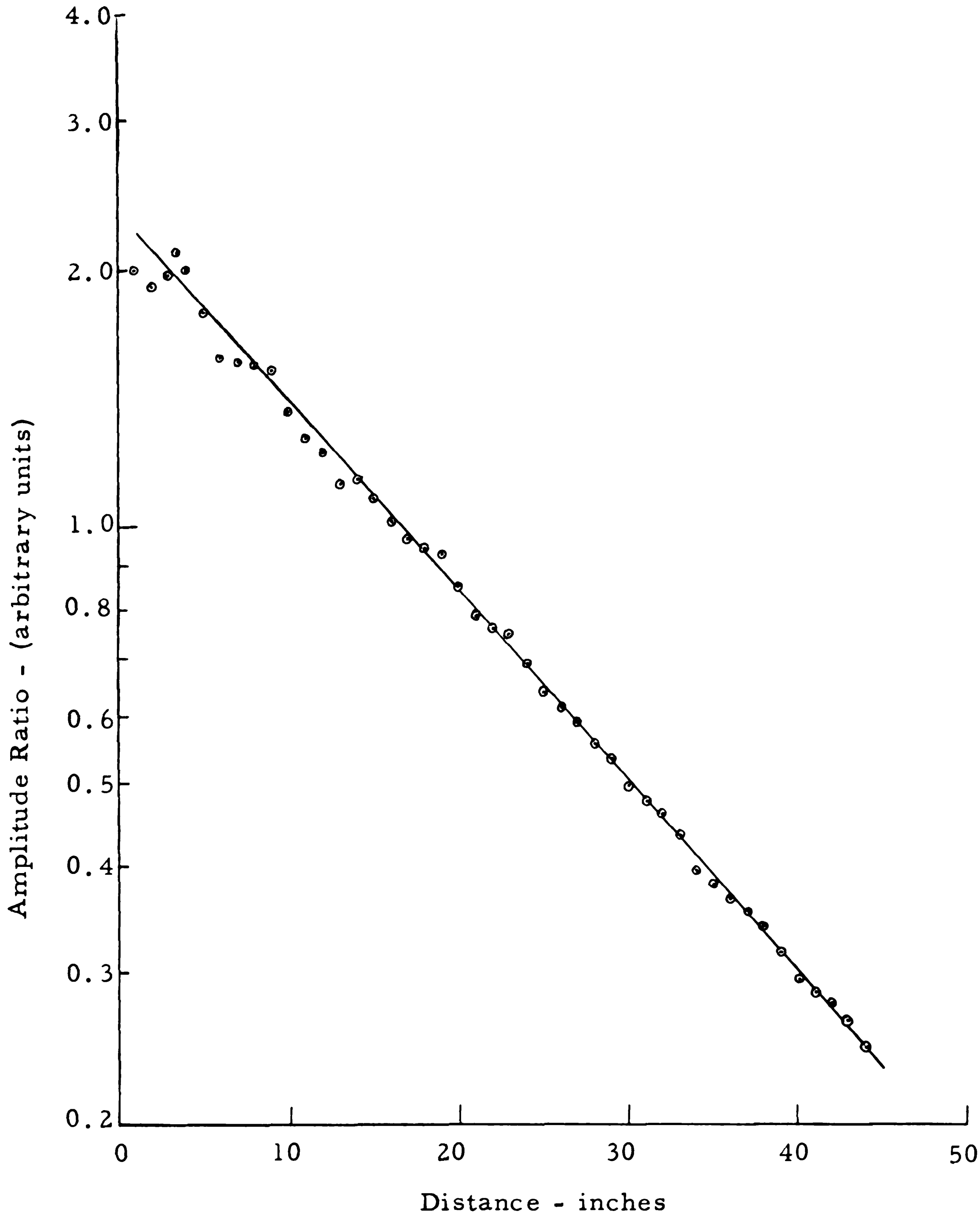

Figure 10. Fiber test on polyethylene at 3000 cps and 75°F. The slope of this curve gives the damping coefficient $\alpha(\omega)$.

Preliminary tests were run maintaining tracking pressure constant at 5 grams but it was found that the results were not sensitive to this pressure and later no great efforts were made to maintain this pressure constant. Checks were also made on slippage between fiber and pick-up and no problems were detected here.

The far end of the fiber was passed over a felt roller and a weight of 0.1 lb. was applied. During a test the roller was then fixed maintaining essentially constant strain during the test.

The pick-up was mounted on the compound rest of a lathe and the cutter on a specially designed bracket on the motor end of the lathe as shown in the photograph, Figure 11. This arrangement allowed a total pick-up travel of 44 inches. The lathe was stripped of everything except the bed, carriage and compound rest. Considerable attention was given to the problem of vibration isolation of the system. A schematic diagram of the apparatus and the associated electronic circuitry is given in Figure 12.

The signal from a Hewlett-Packard, Model 200 CD, Wide Range Oscillator was fed into a high fidelity type 50 watt power amplifier and used to drive the cutter. A Hewlett-Packard Model 400A Vacuum Tube Voltmeter was used to set and maintain constant input voltage to the cutter. The signal from the pick-up was amplified by a Tektronix Type 53/54E preamplifier unit mounted in a Tektronix Type 127 preamplifier power supply. The signal amplitude from the crystal was read by a Ballantine Model 320 True Root Mean Square Electronic Voltmeter. The signal phase difference was compared directly with a Type 320-AB Phase Meter manufactured by Acton Laboratories. The input and output waveforms were monitored visually by an oscilloscope. A Hewlett-Packard Model 523B Electronic Counter was used to maintain the frequency constant within a few cycles per second.

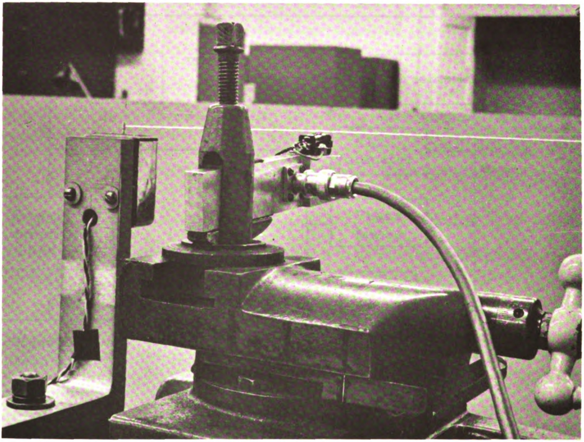

Figure 11. Photograph of the fiber test apparatus. The cutter head is shown on the left and the crystal pick-up in the center on the movable compound rest.

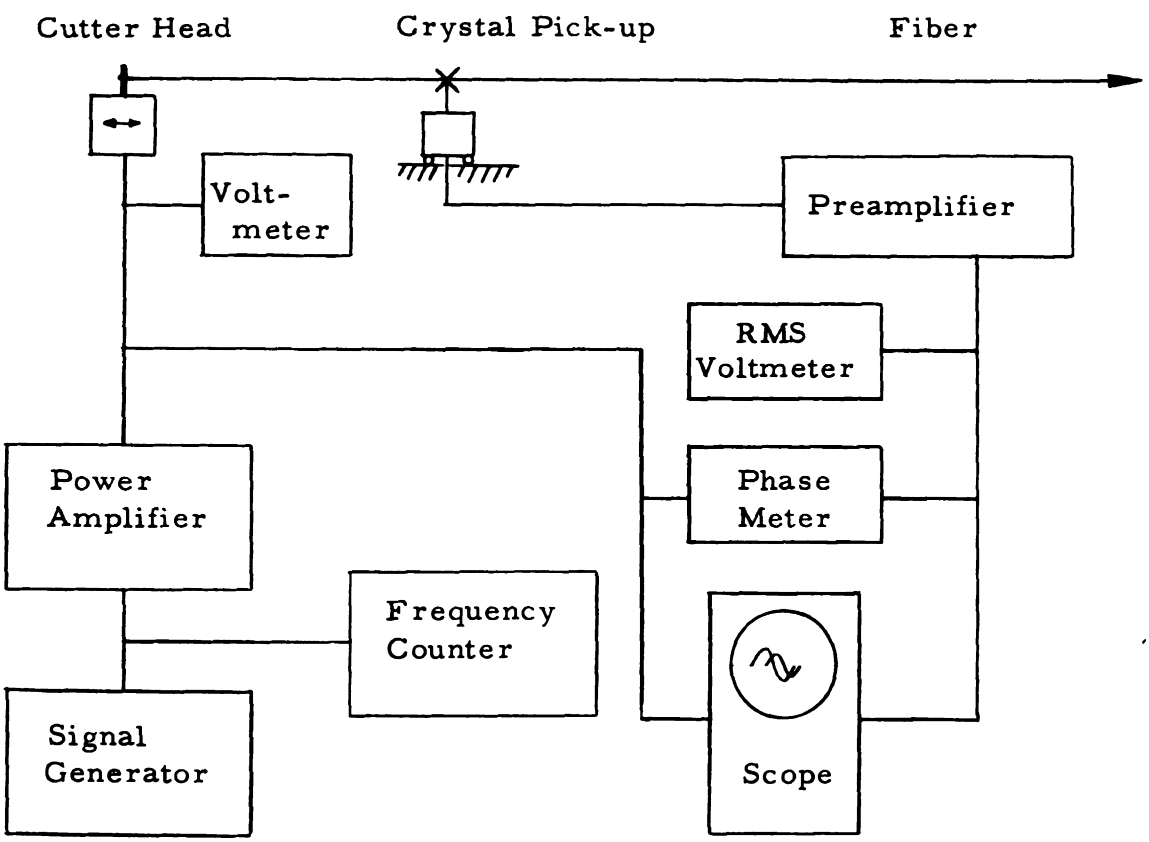

Figure 12. Schematic Diagram of the Fiber Test Apparatus.

The usual experimental procedure was as follows:

1. The equipment was turned on and allowed to stabilize. The fiber was fixed in the constant strain position.

2. The signal generator was adjusted for the desired frequency and amplitude level at the cutter. This level, in general, was set so that at the end of the pick-up traverse, the output level would be just above the minimum detectable level. The level setting used was from about 0.1 volts to 5 volts and was maintained constant throughout each test.

3. The carriage with the crystal pick-up was located properly for the first reading and the RMS voltmeter and phasemeter reading recorded.

4. The fiber was then removed from the pick-up, the carriage moved one inch, the fiber replaced and readings again taken. The process was repeated for the 44 inches of traverse, or in the case of the higher frequencies, until the signal was no longer detectable. A different procedure was used for the very low frequencies.

The data was also reproducible; the percentage difference in velocity values was within 5 percent at the higher frequencies with somewhat more scatter at frequencies below 1000 cps. Values of damping checked to within 1%, however, no attempt was made to secure damping data below 1000 cps where the method was not so accurate. Typical results for a single frequency are given in Figures 9 and 10. The composite damping and velocity curves are given in Figure 13 and Figure 1 respectively and this data is given numerically in Table 1. The damping and phase velocity completely specify the viscoelastic properties of the material.

The assumption of linearity was checked by running tests at the same frequency but with different driving signal voltages. A number of checks were made and over the amplitude levels tested, no significant differences in results were noted.

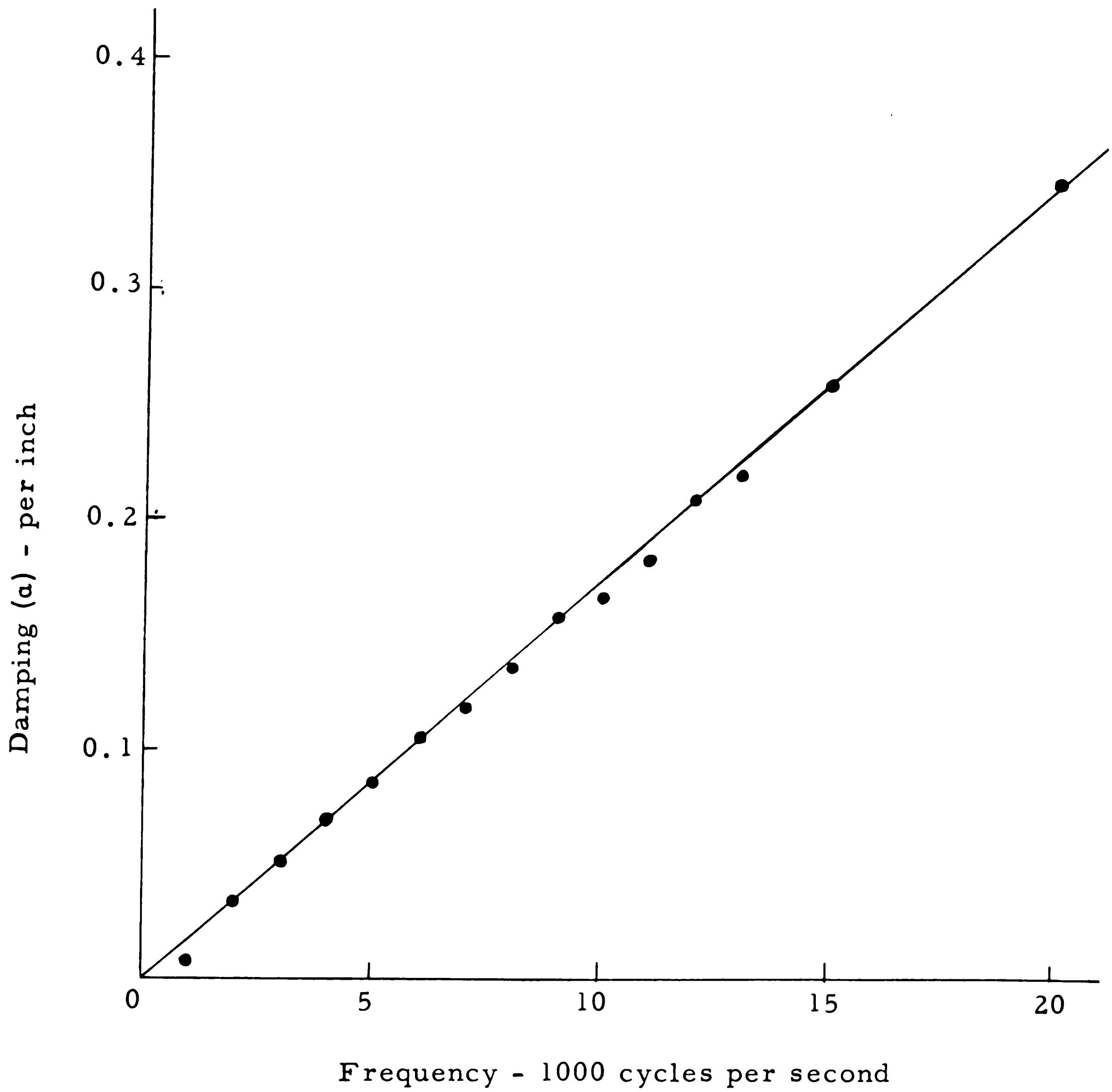

Figure 13. Experimental measurement of damping in polyethylene at 75°F.

Table 1. Phase Velocity and Damping as Measured on Fibers of Polyethylene at 75°F.

Frequency (cps)	Phase Velocity (inches per second)	Damping (per inch)
200	21,998	-
300	24,086	-
400	23,200	-
500	23,775	-
800	25,000	-
900	24,900	-
1,000	25,460	0.0089
2,000	26,374	0.0347
3,000	27,135	0.0514
4,000	27,068	0.0706
5,000	27,027	0.0866
6,000	27,906	0.104
7,000	28,188	0.118
8,000	28,029	0.135
9,000	29,189	0.158
10,000	29,058	0.166
11,000	28,800	0.183
12,000	29,171	0.210
13,000	29,197	0.220
15,000	29,461	0.262
20,000	29,632	0.349

At the lower frequencies it was found that end reflections made it necessary to employ longer fibers. Lengths up to 24 feet were employed and points along the fiber checked by removing the cartridge from the lathe and physically moving it along the fiber in a special jig. At the high frequencies it was found necessary to employ selective electronic filters to remove effects of transverse vibrations from the pick-up signal.

The velocity at zero frequency was determined from static tests using a Pye optical cathetometer. A fiber of polyethylene was suspended from a support and a small initial weight was attached. A gage length of 27.230 centimeters was marked on the fiber and the stress strain curve for loading from 5 to 95 grams in steps of 5 grams was optically determined. No appreciable creep was observed during the time of these tests. By this method a linear relationship was found between stress and strain and the elastic modulus was found to be 12,710 psi. Taking the specific gravity of the material as 0.915, the velocity was computed to be 12,200 inches per second.

APPENDIX III

IMPACT TESTS

The experimental part of the impact problem consists of applying a measured boundary condition in the form of an axial stress to the end of the initially dead viscoelastic bar. The resulting strain is measured as a function of time at various positions down the bar.

The impact tests were made with a modification of the well-known Hopkinson-Davies pressure bar. An analysis of this bar is given by Davies [1948]. Figures 2, 3 and 4 show the experimental apparatus used in the long pulse impact testing.

Magnesium was selected for the striker and transmitter bars. This metal is commercially available in rods and has a low Young's modulus relative to other metals. This implies a larger strain for a given stress, and since we are measuring a low stress level in the magnesium, we thereby increase the sensitivity. The polyethylene bar has a static modulus in the neighborhood of 12,000 psi necessitating extremely low stress levels for reasonable strains. The pressure bars used were 52 inches long and $\frac{1}{2}$ inch in diameter, Dow specification AZ31B. The bars were cut from 12 foot stock and the faces carefully dressed on a lathe. The faces between the striker bar and transmitter bar were slightly rounded to assure an axial impact. A gage station was located 3 inches from the polymer end of the transmitter bar.

Polyethylene rods of various lengths were employed as test material. The minimum length of the polymer bar was determined from the time necessary for reflections from the far end to return and interfere with strain gage readings. With a gage station 32 inches from the impact face a rod 47 inches long was used. The polymer rods were carefully turned on a lathe to 1/2 inch diameter and the faces squared and dressed. On the final test sample, gage stations were established at 2, 12, 22, and 32 inches from the transmitter bar end of the polymer bar. Figure 14 gives the dimensions of the pressure bar system.

A commercial Hyge Shock Tester, type HY-3422, manufactured by Consolidated Electrodynamics Corporation was mounted horizontally and used to propel the striker bar down the impact frame. The device is designed so that at a given gas pressure differential across a seal, the seal is broken and a high pressure is dumped suddenly onto a piston. The piston is accelerated and a piston rod pushes the striker bar. The piston is then hydraulically decelerated allowing the striker bar to move on alone. The acceleration of the piston is easily and accurately varied by setting the pressure level on the low side of the seal. The device has been used in this laboratory to achieve rod velocities of about 7 feet per second up to 50 feet per second. This is actually in the lower velocity capability range of the device. Striker velocities of about 10 feet per second were used in all this work.

The bars were supported by conventional pillow blocks usually used for rotating shafting. A circumferential groove was machined in the shaft seat; a rubber "O" ring was inserted and used to support the bars. Molykote and light grade oil were used as lubricants. A check on the effect of these supports was made on a pulse in a magnesium bar before and after travel through two of these supports. The resulting amplitude of the pulse was within two percent of the original pulse. With exception of one pillow block on the struck end of the polymer rod, the polymer rod was simply placed in the lower part of the blocks with no top supports.

The gages used were Baldwin-Lima-Hamilton Corporation, SR-4, Type FAP-12-12, foil strain gages with a gage length of 1/4 inch.

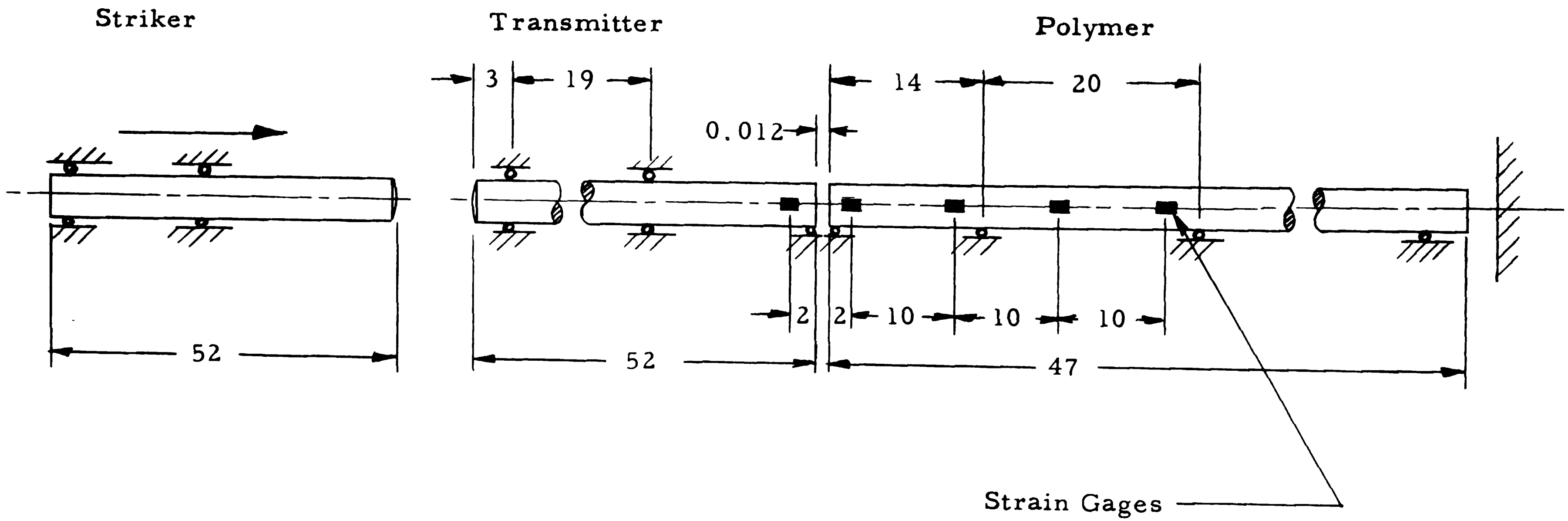

Figure 14. Pressure Bar Dimensions.

To cancel bending stresses the gages were mounted on opposite sides of the rod and in opposite arms of a Wheatstone bridge. Eastman 910 cement was found to be an effective adhesive both for the polymer and magnesium.

The two gages at each gage station were arranged in conventional bridge circuitry using precision resistors in the other two arms. Output was through 0.1 microfarad blocking condensors to the input of the oscilloscope amplifiers. To increase sensitivity, the bridge on the transmitter bar was operated at 12 volts while those stations on the polymer were set at 4 volts each to avoid overheating. Individual wet cells were used in this application.

Output from the transmitter bar bridge was fed to a Tektronix type 53/54E plug-in preamplifier used in a Tektronix Type 532 oscilloscope. The frequency response of the preamplifier is from 0.06 to 60,000 cps with a rise time of 0.06 microseconds.

Output from each polymer bridge was fed into a Tektronix Type 122 Preamplifier which has a frequency response of 0.16 to 40,000 cps. Output from these preamplifiers was fed into two Tektronix Type 53/54C dual-trace plug-in amplifiers used in a Tektronix Type 551 dual-beam oscilloscope. An electronic switch built into the amplifier units allowed the two available oscilloscope beams to separately display output of all four polymer gage stations. The response of these plug-in units is in the megacycle range with a rise time of less than one microsecond. This arrangement allowed all four polymer gage stations to be monitored on a single sweep of the oscilloscope. Both oscilloscopes were triggered from one ammonium dihydrogen phosphate (ADP) crystal mounted on the transmitter bar, three inches in front of the gage station.

Dumont Type 302 oscilloscope cameras were used to record the pulses. Polaroid Pola Pan 400, type 44, film was used with the shutter stopped to f 2.8. Samples of the photographic results are given in Figure 5.

In performing the impact tests the following procedure was generally followed:

1. The two oscilloscopes, the Type 122 preamplifiers and the magnesium strain gage bridge were turned on and allowed to stabilize.

2. The impact end diameter of the polymer bar was checked by micrometer.

3. A gap of 0.012 inches was set between the polymer bar and the transmitter bar. The striker bar was seated firmly against the pusher on the Hyge piston rod.

4. The Type 532 oscilloscope (monitoring the strain in the magnesium bar) was set to sweep at 50 microseconds per centimeter with sensitivity of 0.5 millivolts per centimeter. The oscilloscope was set to single sweep, the camera lens opened and the crystal triggered manually. This records a zero level trace (see Figure 5) on which later was superimposed the Boundary condition trace. The shutter was closed and the single sweep reset.

5. The Type 551 oscilloscope was adjusted to sweep at various rates from 100 to 200 microseconds per centimeter. The sensitivity was set to approximately 10 millivolts per centimeter and the oscilloscope placed on single sweep. The polymer bridges were switched on.

6. Pressure was applied slowly to the Hyge Shock Tester and, just before firing, the camera shutters were opened manually. After firing, the shutters were closed, the Hyge recocked and the bars again positioned for another test. The polymer bar was again checked by micrometer and the bridge voltages recorded.

The voltage calibrator output from the Type 551 oscilloscope was calibrated to within three percent accuracy by a factory representative just prior to testing. This output was photographed on both oscilloscopes set for a normal test run and these photographs used to determine output from the strain gage bridges.

The actual strains were then computed by use of the unbalanced strain gage bridge equation

$$\epsilon = \frac{2}{V_0 F} \Delta V \tag{46}$$

where V_0 is the applied bridge voltage, F is the gage factor for a single gage and ΔV is the change in voltage produced by the strain, ϵ, and measured from the calibrated oscilloscope trace.

The horizontal sweep was calibrated by photographing the marker output from a Rutherford Model B7 Pulse Generator. The marker frequency was monitored by a Hewlett-Packard Model 523B Electronic Counter. By this method the horizontal sweep was calibrated accurately to within one percent across the entire tube face. The photographs were analyzed in a Pye, two-dimensional measuring microscope accurate to 0.01 mm.

To determine the stress boundary condition on the polymer rod, it is necessary to know the Young's modulus of the magnesium since we are measuring the strain in the transmitter bar. This may be determined from the relation

$$E = \rho \, C_0^2 \tag{47}$$

where E is the modulus, ρ is the mass density per unit volume and C_0 is the velocity of sound in the material.

The velocity C_0 was measured by photographing a pulse as it passed two strain gages a known distance apart. Knowing the calibrated sweep speed the velocity could be determined. Using the manufacturer's density of 0.066 pounds per cubic inch and the measured velocity, the dynamic Young's modulus was determined to be 6.63×10^6 psi.

The value of C_0 was checked using an Arenberg ultrasonic pulsed oscillator and identical results were obtained.

The difference in amplitude found initially between computed and experimental strain (a factor of about 2) made the output of the gages suspect. A test was devised to check the amplitude of this gage output against another method of measuring strain. If the striker velocity is known, we may compute the strain from the relationship

$$\epsilon = \frac{V_S}{2C_0} \tag{48}$$

where V_S is the striker velocity and C_0 is the velocity of sound in magnesium.

The striker velocity was measured by a two beam photo cell, the beams separated by a distance of one inch. The output of the cells was amplified and the resulting voltage used to start and stop an electronic counter. The apparatus is similar to that used by Habib [1948]. Knowing the time required for the striker bar to travel one inch, the velocity is determined and the strain may be computed from Equation (48).

The strain computed from Equation (48) was compared with that monitored from the gage station on the transmitter bar as shown in Figure 2. The resulting strain was accurate within 10%; the error being attributed to defects in the simple photocell apparatus.

APPENDIX IV

NUMERICAL EVALUATION OF EQUATIONS

Equation (5) for the stress boundary condition and Equation (6) for the strain boundary condition were integrated numerically using the Michigan State University digital computer, MISTIC, a twin to the ILLIAC at the University of Illinois.

An interpretive routine (A1) and the associated subroutines were used in the work. The integrals were all evaluated by the EA1-M subroutine which employs quadrature formula Q66 (see Kunz [1957]). This formula uses a sixth degree polynomial that fits the g(f) values at seven points and then integrates over the six panels between f_0 and f_6. The program is written to then sum these blocks of six panels.

Equations (5) and (6) were actually converted to frequency and integrated over 12 blocks. The frequency increments were chosen to be 100 cps. Hence each program put the integral limits from 0 to 7200 cps. This was found to be sufficient for x = 32 inches but at earlier gage stations it was found it was necessary to integrate to as high as 21,600 cps. The 100 cps frequency increment was selected when it was shown the results differed little from use of a larger increment.

In each case the damping was expressed in the form of Equation (7) and introduced into the integrals of Equations (5) and (6). The phase velocity for each 100 cps of frequency was stored in the machine and the appropriate value selected by the computer in evaluating the integrand ordinates.

To speed up the calculation it was found desirable to evaluate $\bar{\sigma}_R$ and $\bar{\sigma}_I$ (see Equation (5)) analytically. This was possible since $\sigma(0, t)$

was experimentally shown to be accurately represented by a Heaviside step function, $\sigma_0 H(t)$. Since these integrals are divergent for the usual step function, a pulse of the form

$$\begin{aligned} \sigma(0,t) &= \sigma_0[H(t) - H(t-\beta)] && 0 \leq t \leq \beta \\ &= 0 && t > \beta \end{aligned} \tag{49}$$

was used.

σ_0 is the average height of the stress pulse and β was the approximate length of the experimental pulse. σ_0 was found to be 335 psi and β was chosen to be 500 microseconds. Of course the results are now only significant for the first 500 microseconds of time after the pulse reaches a particular gage station.

With the above assumptions A(f) and B(f) of Equation (5) now become

$$\begin{aligned} A(f) &= \frac{\sigma_0}{2\pi\rho f c^2} \left[\sin 2\pi f\beta + \frac{kc}{\pi} (\cos 2\pi f\beta - 1)\right] \\ B(f) &= \frac{\sigma_0}{2\pi\rho f c^2} \left[\frac{kc}{\pi} \sin 2\pi f\beta - (\cos 2\pi f\beta - 1)\right] \end{aligned} \tag{50}$$

where k here is the slope of the damping versus frequency curve. The results of the integration are plotted in Figure 6 and compared with the corrected experimental values.

Equation (6) for strain was evaluated in a similar manner by choosing a Heaviside step strain function

$$\begin{aligned} \epsilon(2,t) &= \epsilon_2 [H(t) - H(t-\beta)] && 0 \leq t \leq \beta \\ &= 0 && t > \beta \end{aligned} \tag{51}$$

which approximates the strain measured experimentally at x = 2 inches.

Time zero is measured from the time the pulse reached x = 2 inches. The strain is then computed for x = 12, 22, and 32 inches. ϵ_2 was taken as 3397 microinches per inch. The results are given in Figure 7 and compared with the uncorrected experimental strain gage readings.

The integral used by Kolsky [1956], Equation 40, is quite similar to Equations 5 and 6. This integral was programmed and compared with Kolsky's computed results. Values for the phase velocity and attenuation were taken from Kolsky's 1956 paper. The results, shown in Figure 15, show excellent agreement and serve as a check on the accuracy of the computer program.

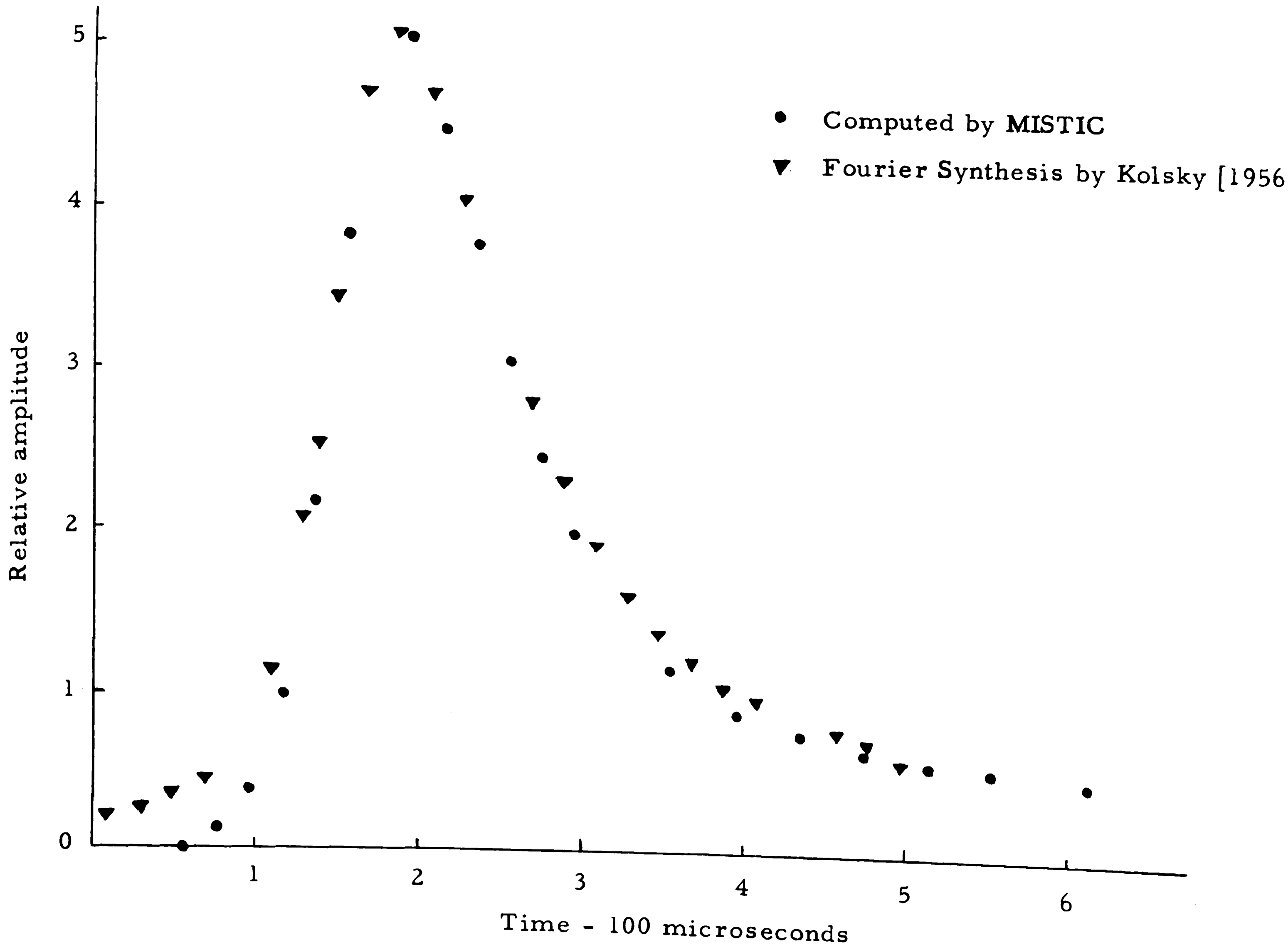

Figure 15. Comparison of computer program with computed curve of Kolsky [1956]. The above curves represent solutions of Equation 40 at $x = 60$ cm.

APPENDIX V

STRAIN GAGE TESTS

Comparison of the original computed and experimental results showed good agreement in wave shape. However, the amplitude of the computed results were higher by a factor of about two from the experimental results. The computer program, using the $x = 2$ inch strain boundary condition, gave excellent amplitude agreement with the experimentally measured strain. Hence it was felt that perhaps the polymer gages were not correctly calibrated for service on polyethylene and were uniformly reading a value lower than the true strain.

To check the indicated strain from the gages, short samples were cut from the polyethylene sample bars with the strain gages already mounted. These samples were tested at various strain rates in compression in an Instron Tensile Testing Instrument. The chart of the recorder built into this machine is driven synchronously at a wide variety of speed ratios with respect to the crosshead, thus enabling measurements of sample compression to be made with a large choice of magnification factors. Hence the strain may be independently recorded.

The two pages on each specimen were installed in a bridge circuit with two 120 ohm precision dummy resistors. The output from these gages was brought into a Type Q Transducer and Strain Gage Plug-in Unit mounted in a Tektronix Series 530 oscilloscope. A very slow single sweep of about one centimeter per second was used and the trace photographed with a Polaroid camera. The system was calibrated by the built-in calibration device in the Q unit and the displacement photographed. The photographs were measured using the Pye measuring instrument previously discussed.

The experimental procedure was as follows:

1. The sample was carefully measured, lubricated and placed in the Instron machine.
2. A small preload of about 3 kg. was put on the specimen.
3. The trace was triggered by pushing the reset button on the oscilloscope and the recorder chart was started.
4. The camera shutter, set on "time," was opened and the Instron started.
5. The machine was stopped, the camera shutter closed and the photograph removed.

Separate checks were made on a number of samples to check for possible barreling effects. Careful measurement by micrometer over the range of strains used showed no such effects.

The results of these tests are shown in Table 2 below.

Table 2. Tests on Output of Strain Gages on Polyethylene.

Strain Rate (cm/min)	Recorder Strain (microinches/inch)	Initial Length (inches)	$\frac{\text{Recorder Strain}}{\text{Gage Strain}}$
0.02	2400	1.539	2.55*
0.02	4810	1.539	2.56*
0.05	6897	1.3978	2.530
0.05	7434	1.5362	2.544
0.5	7039	1.3978	2.219
0.5	7039	1.3978	2.254
1	8344	1.3978	2.202
1	7039	1.3978	2.114
1	13,857	1.3978	2.29
1	18,589	1.3978	2.20

*The strain was monitored visually on the oscilloscope.

It is seen from Table 2 the ratio of true strain and gage strain is relatively independent of strain rate and strain amplitude. The values read at the high strain rate were averaged and a correction factor of 2.20 wasused in plotting the experimental data of Figure 6. The uncorrected data is shown in Figure 7.

ROOM USE ONLY